JGR Solid Earth

RESEARCH ARTICLE
10.1029/2020JB020472

Deep Structure of the Grenada Basin From Wide-Angle Seismic, Bathymetric and Gravity Data

Crelia Padron[1,2], Frauke Klingelhoefer[2], Boris Marcaillou[3], Jean-Frédéric Lebrun[4], Serge Lallemand[5], Clément Garrocq[5], Mireille Laigle[3], Walter R Roest[2], Marie-Odile Beslier[3], Laure Schenini[3], David Graindorge[6], Aurelien Gay[5], Franck Audemard[7], Philippe Münch[5], and the GARANTI Cruise Team

[1]Departamento de Ciencias de la Tierra, Universidad Simón Bolívar (USB), Caracas, Venezuela, [2]Géosciences Marines, Ifremer, ZI de la Pointe de Diable, Plouzané, France, [3]Geoazur, Université Côte d'Azur, CNRS, IRD, Observatoire de la Côte d'Azur, Valbonne, France, [4]Géosciences Montpellier, Université des Antilles, CNRS, Université de Montpellier, Campus de Fouillole, Pointe-à-Pitre, Guadeloupe, France, [5]Géosciences Montpellier, CNRS, Université de Montpellier, Université des Antilles, Montpellier, France, [6]Laboratoire Géosciences Océan, CNRS-UBO-UBS, Université Bretagne Pays de Loire (UBL), Brest, Institut Universitaire Européen de la Mer, Plouzané, France, [7]Venezuelan Foundation for Seismological Research, Caracas, Venezuela

Abstract The Grenada back-arc basin is located between the Aves Ridge, which hosted the remnant Early Paleogene "Great Caribbean Arc," and the Eocene to Present Lesser Antilles Arc. Several earlier studies have proposed different modes of back-arc opening for this basin, including N-S and E-W directions. The main aim of this study is to constrain the circumstances leading to the opening of the basin. Three combined wide-angle and reflection seismic profiles were acquired in the Grenada basin. The final velocity models from forward travel time and gravity modeling image variations in thickness and velocity structure of the sedimentary and crustal layers.

The sedimentary cover has a variable thickness between 1 km on top of the ridges to ~10 km in the basin. North of Guadeloupe Island, the crust is ~20 km thick without significant changes between Aves Ridge, the Grenada basin, and the Eocene and present Lesser Antilles arc. South of Guadeloupe Island the Grenada basin is underlain by a oceanic crust of mainly magmatic origin over a width of ~80 km. Here, the western flank of the Lesser Antilles Arc, the crust is 17.5-km thick. The velocity structure of the Lesser Antilles Arc is typical of volcanic arcs or oceanic plateaus. West of the basin, the crust thickens to 25 km at Aves Ridge in an 80–100 km wide arc-ocean transition zone. The narrowness of this transition zone suggests that opening might have proceeded in a direction oblique to the main convergence. Opening probably was accompanied by moderate volcanism.

Plain Language Summary In this study, we investigated the formation of the Grenada Basin, located west of the Lesser Antilles island arc. These types of basins typically open behind subduction zones, where one tectonic plate is moving underneath another plate. We deployed instruments on the seafloor to record acoustic signals made using pressured air in an array towed behind the ship. This method allowed us to image the sediments and crustal layers along the three profiles of our study. We find that the structure of both the eastern and western margin of the basin are similar in their physical properties, that volcanism was widespread during basin opening, and the southeastern part of the basin is underlain by crust typically found in oceans. More research is needed to explore the direction of opening and the extent of the oceanic-type crust underneath the modern island arc.

This article is a companion to Garrocq et al. (2021), https://doi.org/10.1029/2020JB020466.

Key Points:

- Wide-angle and gravity data were acquired along three profiles in the Grenada basin during the GARANTI cruise in 2017
- Crustal thickness at Aves ridge and the Lesser Antilles arc is between 21 and 27 km and velocities are compatible with other volcanic arcs
- A 80-km-wide region in the south of the basin is underlain by oceanic crust

Supporting Information:

- Supporting Information S1

Correspondence to:
C. Padron,
crelia.padron@gmail.com

Citation:
Padron, C., Klingelhoefer, F., Marcaillou, B., Lebrun, J.-F., Lallemand, S., Garrocq, C., et al. (2021). Deep structure of the Grenada Basin from wide-angle seismic, bathymetric and gravity data. *Journal of Geophysical Research: Solid Earth*, *126*, e2020JB020472. https://doi.org/10.1029/2020JB020472

Received 26 JUN 2020
Accepted 17 OCT 2020

1. Introduction

At the Lesser Antilles subduction zone, the North and South American plates are subducting underneath the Caribbean plate (Figure 1). The crescent-shaped Grenada back-arc basin is located between the Aves Ridge, which hosted the remnant Early Paleogene Great Caribbean Arc, and the Late Eocene to Present Lesser Antilles Arc (LAA). The N-S-trending Aves Ridge extends between Virgin Islands and Venezuela, rising 2,000–3,000 m above the surrounding seafloor and bounding to the west the Grenada Basin. The "Great Arc of the Caribbean" of which Aves Ridge is a remaining expression, is a volcanic arc that developed about 135 Ma ago at the subduction of the future Caribbean plate and the Proto-Caribbean Ocean (Boschman

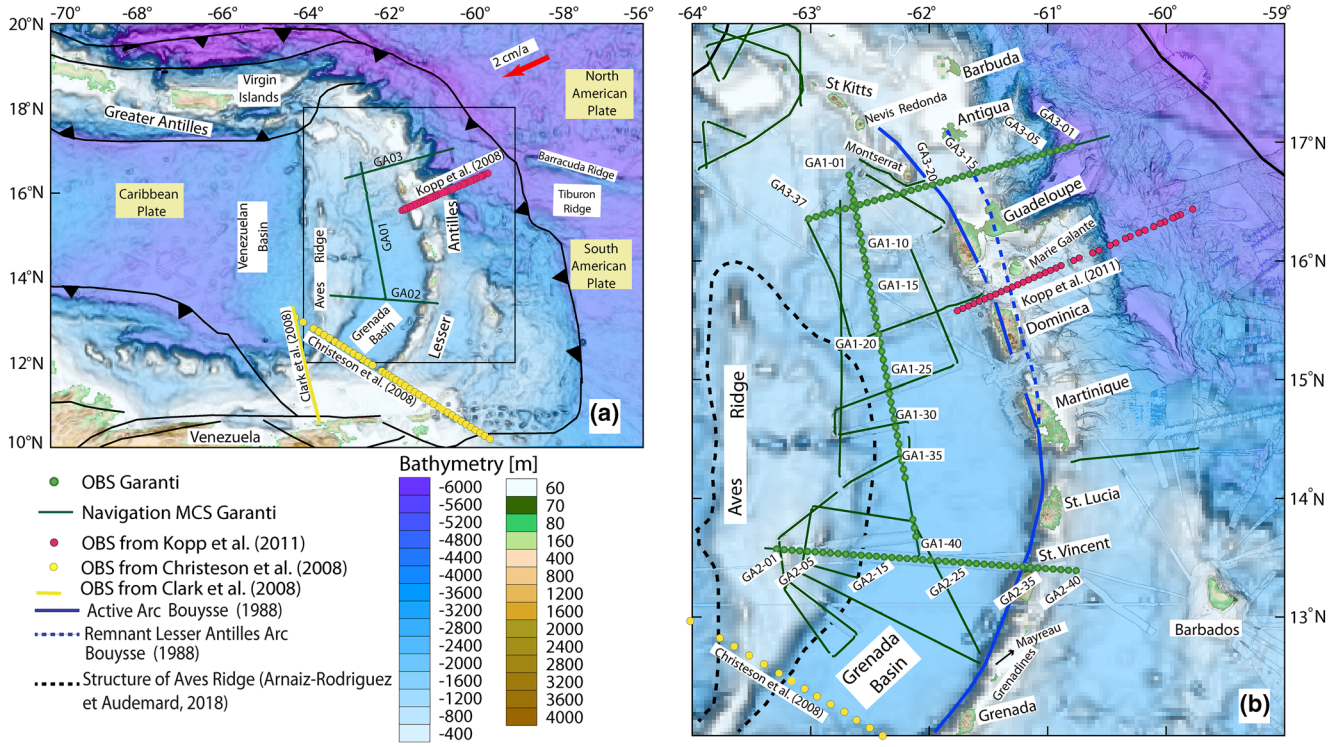

Figure 1. (a) Regional bathymetric map showing the location for wide-angle seismic lines acquired during the Garanti Cruise (Lebrun & Lallemand, 2017). (b) Bathymetry of the study area including the position of the wide-angle profiles (green dotted lines) and multichannel reflection profiles (green thin lines). The bathymetric chart displays a compilation of data from ETOPO1 (doi:10.7289/V5C8276M), and previous cruises. Red circles mark the position of seafloor instruments from Kopp et al. (2011). Yellow circles and line mark the position of seafloor instruments from Christeson et al. (2008) and Clark et al. (2008), respectively.

et al., 2014; Burke, 1988). Arc magmatism then shifted to the Limestone Caribbees in the middle Eocene and is concentrated today at the Lesser Antilles Volcanic arc (Figure 1).

Most recent geophysical studies in the Lesser Antilles focused on the forearc area and the oceanic domain (e.g., Laurencin et al., 2017, 2018; Paulatto et al., 2017). In these areas, intense subduction-related tectonic deformation often overprints initial basin structure, hampering detailed investigations about their formation. Therefore, studying back-arc basins, where basement, sedimentary layers and possibly the whole lithosphere are less deformed, provides complementary information about formation and tectonic evolution of subduction zones.

The Lesser Antilles back-arc area has a complex structure, which includes the remnant Paleogene Great Caribbean Arc (Burke, 1988), the ~670-km-long and up to 100-km-wide Aves Ridge and the deep and flat Grenada Basin, bounded to the North of 16°N by a shallower and hummocky seafloor. Previous investigations with sparse seismic probing resulted in various models for the tectonic origin of this area: eastward jump of the volcanic arc trapping an Atlantic ocean fragment (Donnelly, 1975; Malfait & Dinkelman, 1972), Wernicke-type simple shear extension (Arnaiz-Rodríguez & Audemard, 2018), forearc spreading and flexural subsidence (Aitken et al., 2011), back-arc spreading with various extension direction, east-west (Audemard, 1993, 1998, 2009; Bird et al., 1999; Tomblin, 1975), northeast-southwest (Bouysse, 1988) (Figures 2a–2c), north-south (J. L. Pindell & Barrett, 1990), and northeast-southeast (J. L. Pindell & Kennan, 2009) (Figure 2d). Other propositions include the existence of oceanic crust underneath the modern arc either formed within a forearc (Aitken et al., 2011) (Figure 2e) or in a back-arc setting (Allen et al., 2019) (Figure 2f). These studies assume a portion of oceanic crust surrounded by a thicker crust of volcanic or continental origin. However, none of these interpretations are supported by solid constraints about the nature, thickness, structure and deformation of the basement at depth beneath the ridge and the basin.

During the Garanti cruise, we acquired 3 wide-angle seismic lines, 30 multi-channel reflection seismic lines, bathymetry and additional magnetic and gravity shipboard data (Lebrun & Lallemand, 2017) in order to

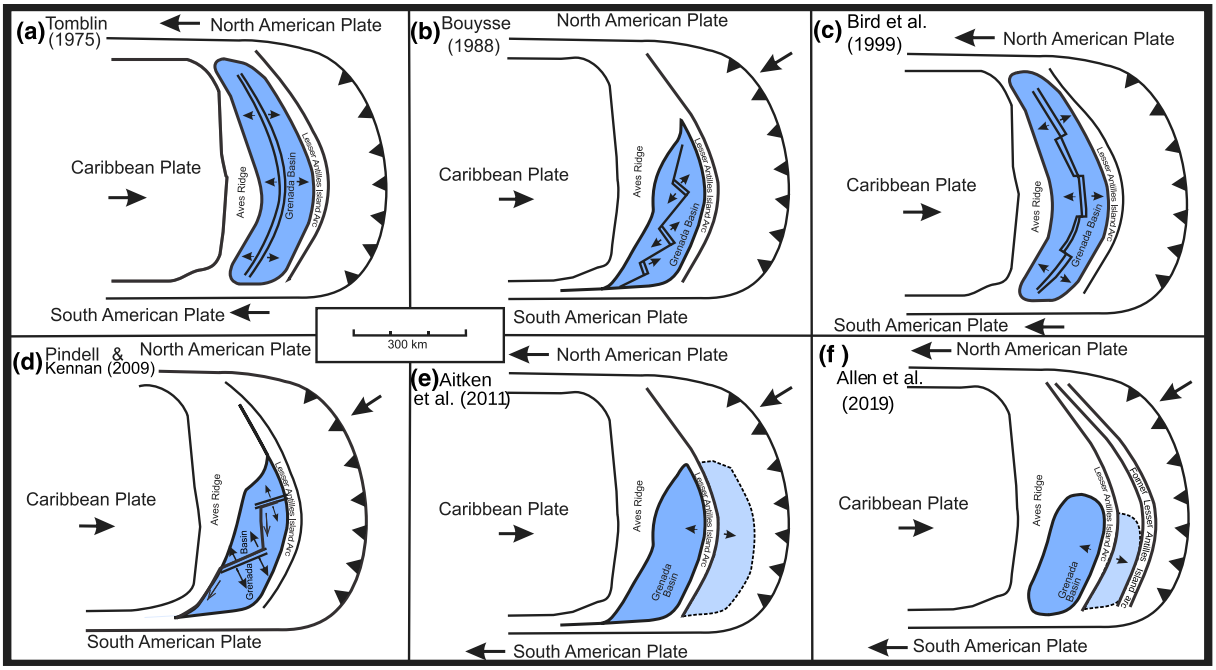

Figure 2. Models of Grenada back-arc basin opening proposed by earlier studies. (a)–(c) are modified from Bird et al. (1999), (d) is cartoon model for the opening of J. L. Pindell & Kennan (2009), (e) is schematic summary corresponding to the model of Aitken et al. (2011) and (f) to the model of Allen et al. (2019).

study the sedimentary and deep crustal structures of the Grenada Basin and the eastern Aves Ridge (Figure 1). The project aims at deciphering the tectonic origin and evolution of the Grenada Basin, the chronology of volcanic arc migrations and the vertical movement that likely triggered emergence phases and land-bridges formation.

In this study, based on wide-angle data, we provide constraints about lateral variations in basement thickness and velocity structure in the Lesser Antilles back-arc, and to a lesser extent in the arc and forearc domain, constraining for the first time the extent of oceanic crust in the Grenada Basin and shedding light on the structure and compositions of the basin's margins.

2. Previous Work

The first wide-angle seismic studies of the Grenada basin were undertaken in the 1950s (Ewing et al., 1957; C. Officer et al., 1959). At that time, the Moho depth at Aves Ridge was determined to be at a minimum of 15 km below sea level, thinning in the Grenada trough. The authors propose a volcanic origin for a 1–2 km thick layer identified on top of the crust over most of the study region. Dredges taken from the southern end of the Aves Ridge yielded limestones, marls, and cherts, as well as granodiorite and andesites (Bouysse et al., 1985; Fox et al., 1971; Neill et al., 2011). Dredged carbonate samples showed that parts of Aves Ridge were in shallow water during the Eocene and Early Miocene and then subsided by 400–1,400 m.

A first hypothesis was that the Grenada basin is a piece of Atlantic crust trapped after an eastward jump of the subduction from Aves Ridge to the active arc location (Kearey, 1974). Based on reflection seismic data and gravity modeling, the Aves Ridge was proposed to be an island arc deactivated when subduction stepped back to its present day position at the LAA (Bunce et al., 1970; Kearey, 1974; Tomblin, 1975). Later, it has been interpreted as a back-arc basin after rifting of the Lesser Antilles island arc, however with a highly variable extent of oceanic crust and accretionary direction (Audemard, 1993; Bird et al., 1999; Bouysse, 1988; J. L. Pindell & Barrett, 1990; J. L. Pindell & Kennan, 2009; Tomblin, 1975) (some examples in Figures 2a-2d).

Although it was generally agreed that the Grenada Basin was formed as a back-arc basin in Cenozoic times after rifting of the Lesser Antilles island arc, different propositions regarding the opening direction, eg., east-west (Tomblin, 1975), northeast-southwest (Bouysse, 1988), diffuse (Bird et al., 1999), or northwest-southeast (J. L. Pindell & Kennan, 2009) were published (Figures 2a–2d); and even radial for a much larger back-

arc basin stretching between Saba Bank and Falcón Basin (Audemard, 1993, 1998, 2009). Later wide-angle seismic work revealed a Moho depth of up to 40 km beneath Aves Ridge and around 35 km underneath St. Vincent (Boynton et al., 1979). Moho depth in the Grenada and Tobago trough was determined to be 21 and 25 km and characterized by crust of modified oceanic type. In the Tobago basin, located east of the LAA, sediments were deposited and built the Barbados Ridge (Westbrook, 1975).

Speed et al. (1993) presented a study of rocks exposed on Grenada and the Grenadine Islands of the southern Lesser Antilles arc platform showing that the oldest rocks exposed here date from the early to middle Eocene and originated from sea-floor spreading that created the Mayreau Basalt. W. White et al. (2017) based on geochemistry studies of a basalt from Mayreau concludes that the basalt is consistent with a formation in a backarc spreading environment and therefore consistent with the interpretation of Speed et al. (1993).

A 568-km-long wide-angle seismic profile crossing the active island arc, the remnant Great Caribbean Arc and the Grenada and Tobago basins was acquired showing that the crust at Aves Ridge and the active arc have similar velocities and crustal thicknesses, and are probably of comparable origin (Christeson et al., 2008). Based on this transect, other reflection seismic lines and fault restoration, the shortening in the Grenada Basin was estimated to be at least 5 km in the southern part of the basin, reducing to zero in the North, where the influence of the oblique convergence between the Caribbean and South American plate is minimal (Aitken et al., 2011). The symmetry of the sedimentary sequences also implies that the Grenada and Tobago basin originally formed one single forearc basin which was then divided by the intrusion of the active LAA (Aitken et al., 2011; R. C. Speed & Walker, 1991) (Figure 2e). Clark et al. (2008) presented wide-angle velocity modeling results from a profile located at ∼64°W longitude (Figure 1a). The crustal structure of the remnant Great Caribbean arc section of this profile is characterized by a crustal thickness between 21 and 28 km and a significant heterogeneity in the velocity structure.

Two wide-angle seismic (WAS) profiles crossing the forearc and active and remnant LAA north and south of Dominica Island, and a dense Multi-Channel Seismic (MCS) profile grid centered on the forearc were acquired during two seismic cruises (Evain et al., 2013; Kopp et al., 2011; Laigle et al., 2013). In the study region, the arc and forearc crust is about 27 km thick, probably of felsic to mafic composition and can be subdivided into three layers (Kopp et al., 2011). The rather constant thickness and seismic structure of the crust across this 100-km-wide arc and forearc domain conducted the authors to consider this portion as being a remnant of the Caribbean oceanic plateau.

Recently, based on magnetic data, passive and wide-angle seismic data, a three phased development of the Grenada basin has been described (Allen et al., 2019). The authors suggested that a ridge jump transferred the volcanic activity from the Great Arc of the Caribbean along the Aves Ridge to the today remnant LAA, which is called “limestone Caribbees” in the North. Subsequently, a second arc jump westward, away from the subduction led it to its present day position (Allen et al., 2019). In their proposition, oceanic crust is underlying the Grenada Basin as far north as Martinique island (Figure 2f). However, further north, crustal characteristics imply a 15–30 km thick crust (Arnaiz-Rodriguez et al., 2016), that excludes the presence of oceanic crust.

3. Method and Results

3.1. Data Acquisition and Quality

During the Garanti cruise, we deployed 40 ocean-bottom seismometers (OBS) from the Universities of Nice and Brest together with the deep penetrating multi-channel reflection seismic system of Ifremer to acquire three regional combined wide-angle and reflection seismic profiles. The reflection seismic equipment consisted of a 4.5 km solid-type digital streamer including 360 hydrophones with a 6.25 m trace interval and a 6,473 in^3 tuned seismic airgun array with individual gun sizes between 250 and 550 in^3. Shooting was executed every 60 s, leading to a trace spacing of ∼150 m in the seismic sections that were acquired at a ship speed of 5 knots. All seafloor instruments recorded four channels (hydrophone and three geophone channels) at a 4 ms or 10 ms interval and reflection seismic data were recorded using a 2 ms interval.

After recovery of the seafloor instruments, the time drift was measured by comparison with satellite time and the data were downloaded, and subsequently corrected for time drift and formatted. Drift from the

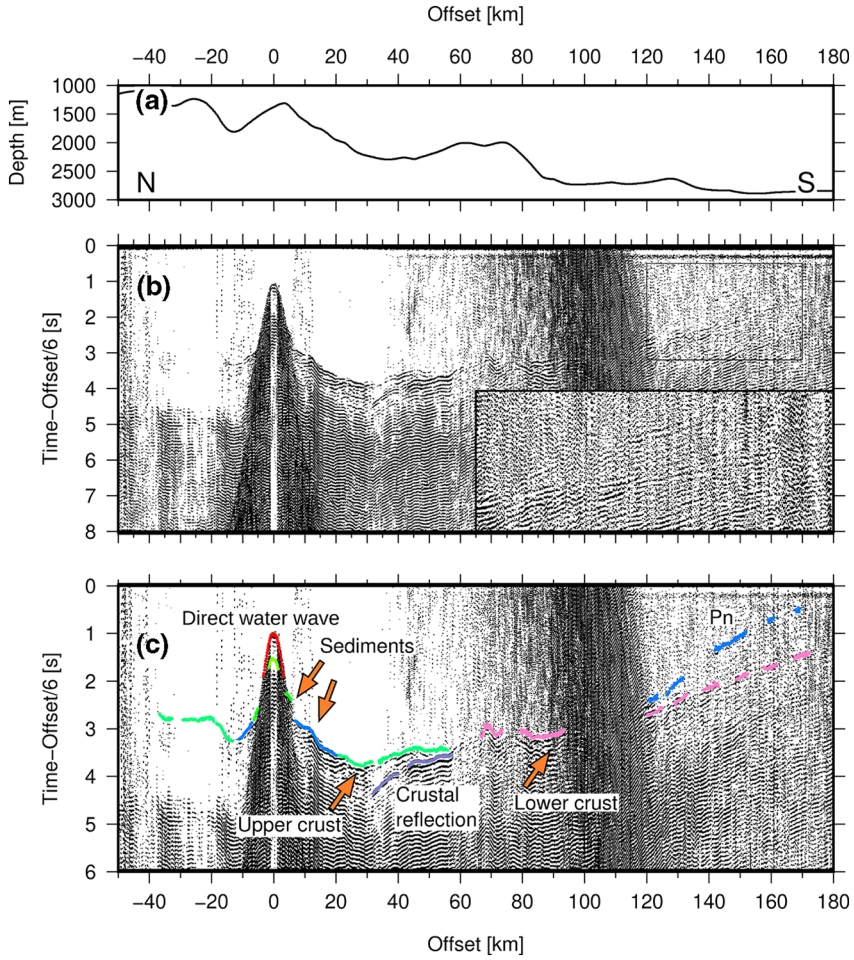

Figure 3. Seismic section OBS 10 on profil GA01. (a) Seafloor bathymetry from shipboard data along the data sections. (b) Bandpass filtered data (Corner frequencies 3–5–24–36 Hz) of the OBS 1–10 (location in Figure 1). Inset shows zoom indicated by black frame. (c) Bandpass filtered data of the OBS 1–10 with travel time picks overlain. A scale proportional to the offset has been applied and main phases are annotated. Pn = turning rays from the upper mantle.

deployment position during the descent to the seafloor was corrected using direct arrivals from the shots. In detail, 39 OBS were successfully deployed along the profil GA01, 40 along the profil GA02, and 37 along the profil GA03. The data quality is generally high on the vertical and hydrophone channels, especially for instruments located far from the coast in deep water, with most instruments having recorded arrivals to offsets greater than 100 km (Figures 3–5). Additional information on the data quality is given in electronic S1. For more detailed analysis of the data quality the original shotgathers in standard SEGY format are accessible (https://doi.org/10.17882/74223).

The reflection seismic data were quality controlled using Ifremer's "SolidQC" software, and a first processing on Geovation CGG software included resampling to 4 ms, anti-alias filtering, multiple suppression by surface-related multiple elimination, predictive convolution, velocity analysis, stack and water-velocity migration (for a more detailed description see the companion manuscript by Garrocq et al., 2021).

3.2. Wide-Angle Seismic Data Modeling

The wide-angle seismic data were modeled with the "rayinvr" software of Colin Zelt (Zelt & Smith, 1992) and its combined inverse and forward approach. This technique allows to include additional information from reflection seismic and gravity data, as well as geologic data, e.g. from scientific drilling. The first and secondary arrivals on the sea-bottom seismometer data were picked with the help of the "OpendTect" soft-

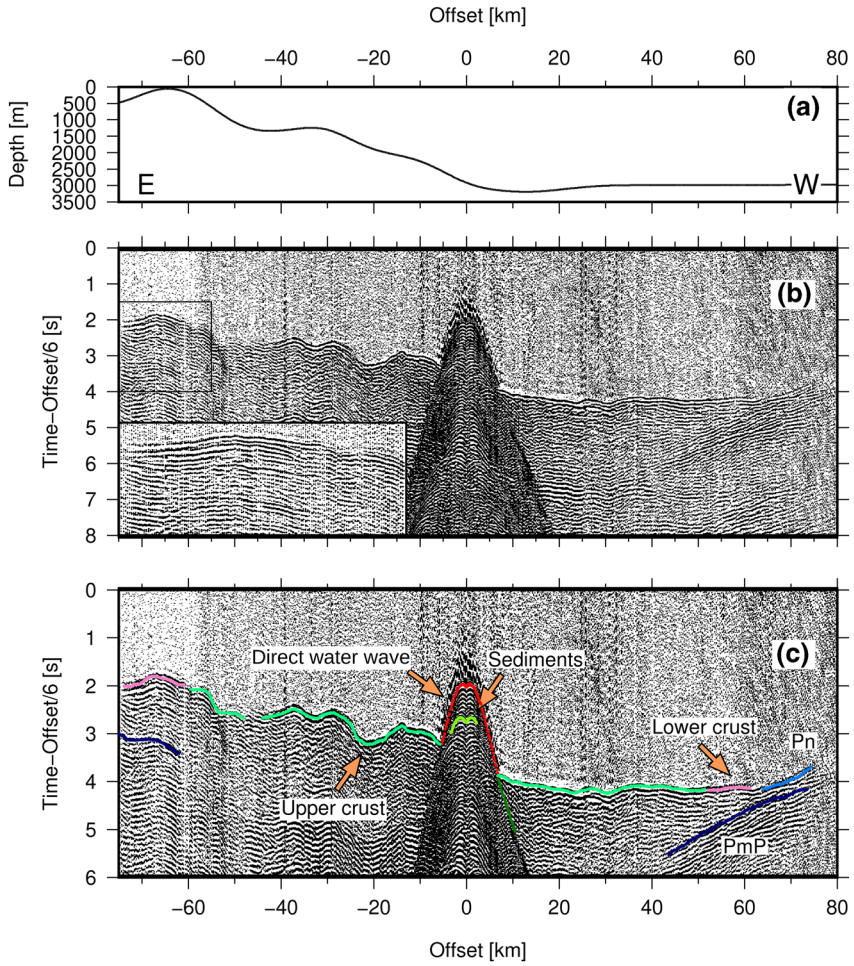

Figure 4. Seismic section OBS 11 on profil GA02. (a) Seafloor bathymetry from shipboard data along the data sections. (b) Bandpass filtered data (Corner frequencies 3–5–24–36 Hz) of the OBS 2–11 (location in Figure 1). Inset shows zoom indicated by black frame. (c) Bandpass filtered data of the OBS 2–11 with travel time picks overlain. A scale proportional to the offset has been applied and main phases are annotated. Pn = turning rays from the upper mantle, PmP = Reflected rays from the Moho.

ware (dGB Earth Sciences). For all sedimentary and basement arrivals of the main layers we picked main reflectors from the coincident reflection seismic sections and converted them to depth using the velocities from seafloor instrument data. The modeling software uses a layer-stripping approach and we modeled layers from top to bottom (Zelt, 1999). The final velocity models along the three profiles include three sedimentary layers, two crustal layers and an upper mantle layer (Figure 6). The GA02 profile includes one additional sedimentary layer, which was not detected along the other profiles. More details about the strategy of travel-time picking and phase organization are given in electronic S1.

3.3. Error Calculations

The error between the picked arrival times and the predicted time from forward modeling indicates the quality of the fit of the velocity model to the data (Figure 7). The combined number of picks and the associated root mean square (rms) residual errors concerning all phases are listed in Table 1.

Resolution measures the number of seismic rays passing through each of the user-defined velocity nodes and it therefore depends directly on the number of nodes in each layer.

It presents the diagonal values of the resolution matrix and should ideally be 1, but values less than one indicates the degree of averaging of the true structure by some of the model parameters. Typically, resolu-

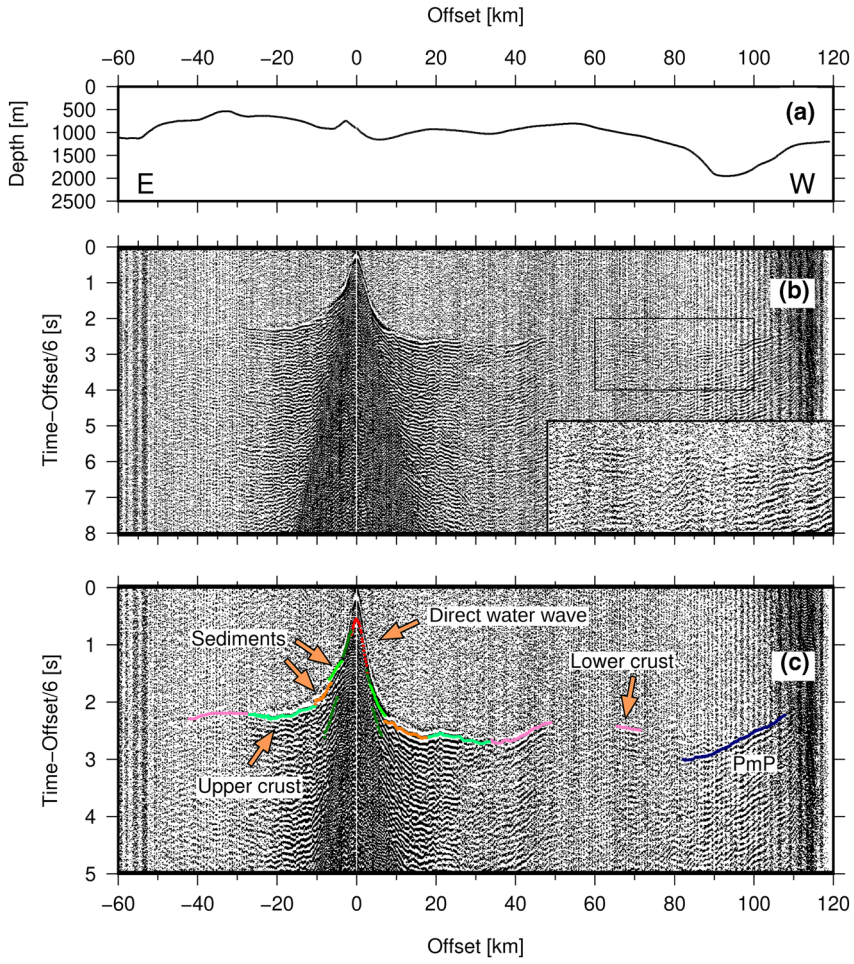

Figure 5. Seismic section OBS 20 on profil GA03. (a) Seafloor bathymetry from shipboard data along the data sections. (b) Bandpass filtered data (Corner frequencies 3–5–24–36 Hz) of the OBS 3–20 (location in Figure 1). Inset shows zoom indicated by black frame. (c) Bandpass filtered data of the OBS 3–20 with travel time picks overlain. A scale proportional to the offset has been applied and main phases are annotated. PmP = Reflected rays from the Moho.

tion matrix diagonals of greater than 0.5–0.7 are said to indicate reasonably well-resolved model parameters (e.g., Lutter & Nowack, 1990; Zelt, 1999). Nodes with a seismic resolution larger than 0.5 can be considered well resolved (see Figures 8a–8c). A layer with only one single node through which all rays pass will thus have a resolution of 1. For this reason, resolution values close to one should be only considered when combined with hit counts (S7b, S8b, and S9b). Resolution is between 0.5 and 1.0 in the sedimentary layers except for the low velocity layer along the profile GA02 (Figure 8b), where no turning rays are produced. The crustal layers generally are well resolved, except at the ends of the profiles, where less rays penetrate. Additional error calculations including smearing factor and ray density are explained and shown in the electronic Text S2 and Figures S7–S9.

3.4. Results From Wide-Angle Seismic Modeling

The velocity models from wide-angle seismic profiles image the sedimentary and crustal structures of the Grenada Basin and its neighboring Great Caribbean and active arcs (Figure 6). The basin basement along GA02 is asymmetric, deepening to the east, and filled with up to 8–9 km of sediments. The crust of Aves Ridge is up to 25 km thick along profile GA02 and the Lesser Antilles active arc has a crustal thickness of about 22–23 km. A similar thickness was modeled for the northern Grenada Basin, west of Guadeloupe Island. A detailed description of each profile will be given in the following subchapters. Lateral variations of the crustal structure and their implications in terms of crustal signature are discussed in Section 4.

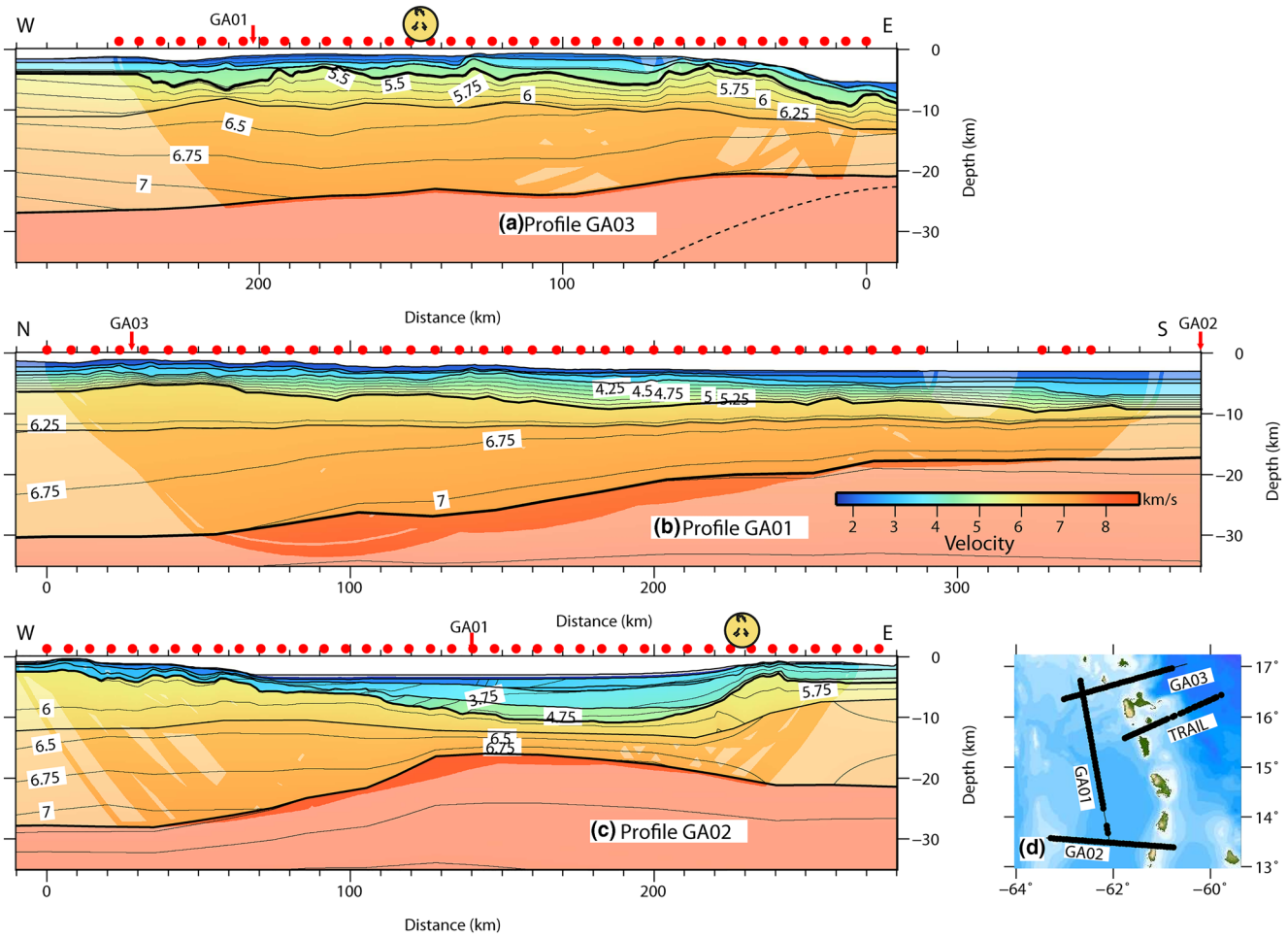

Figure 6. Final velocity models of (a) GA03, (b) GA01 and (c) GA02 profiles from forward modeling with velocities contoured every 0.25 km/s, (d) position of the wide-angle profiles. All regions not constrained by rays from the modeling are shaded but might be constrained by gravity modeling. Red circles mark the position of OBS along the profile, volcano symbols mark the presently active volcanic arc axis and vertical exaggeration is 1:5. The dotted black line in (a) symbolizes the probable location of the top of the subducted slab as extrapolated from MCS data (Laigle et al., 2013).

3.4.1. Profile GA01

Model GA01 is 360 km long and includes three sedimentary layers with Vp of 1.8–2.2 km/s, 2.6–2.7 km/s, and 3.3–3.5 km/s, from top to bottom. Underneath, a supra-crustal layer with Vp of 4.0–5.5 km/s possibly corresponds with metamorphosed volcano-sedimentary, volcaniclastic, and/or altered igneous rocks, above the crust. These 1–3-km-thick layers overall thicken from 3 km in the north to 7 km in the south (Figure 9a). Crustal thickness along the north-south trending profile GA01 varies between 23 km in the north and 8–10 km in the south. The crust is divided into an upper layer with Vp ranging from 6.0 to 6.3 km/s and a lower layer with velocities of 6.5–6.9 km/s in the north increasing to 6.7–7.1 km/s in the south. The ratio of crustal thickness between the upper and the lower crustal layer changes only slightly from the north to the south: in the north the upper crustal layer is about ⅓ of the thickness of the lower crustal layer whereas in the south where it is ¼ of the thickness. The East-West trending lines GA03 and GA02 cross GA01 at the northern and southern ends respectively, where the sampling by crossing rays is poor. Therefore, some misfits occur for the deeper interfaces at those crossing points.

3.4.2. Profile GA02

The velocity model of profile GA02 is 280 km long and images an asymmetric Grenada basin with the basement top deepening from 7 km in the West to over 10 km in the East. Above the crust, the volcaniclastic and sedimentary layers overall thicken from four to more than 7 km, beneath a flat seafloor (Figure 10a). On the eastern flank of the Aves Ridge, these layers thin to less than 3 km. The underlying ~25 km-thick crust is

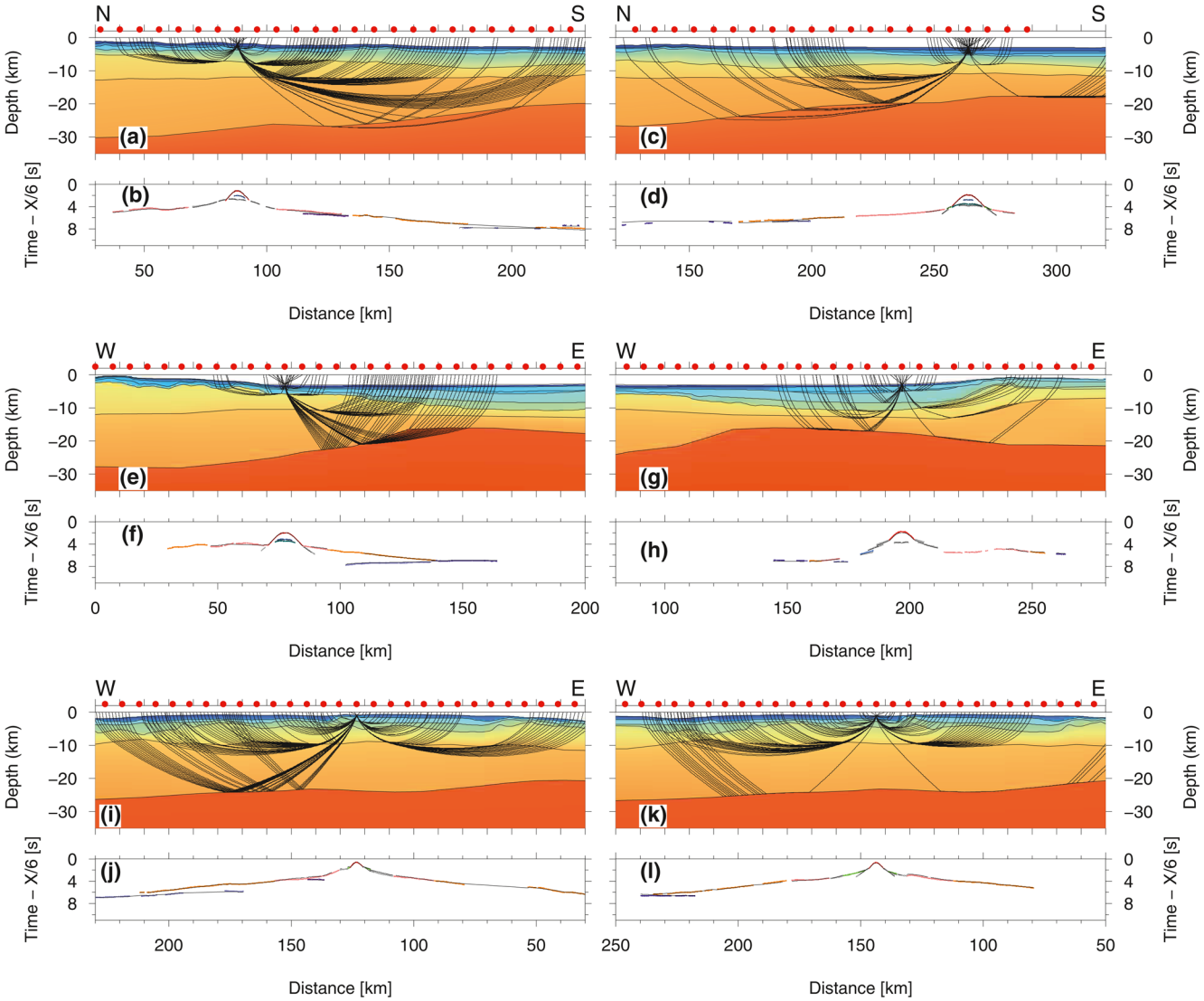

Figure 7. Model layers and ray-paths of every 10th ray (panels a, c, e, g, i, and k) corresponding to travel-time picks and predicted arrivals (black lines) (panels b, d, f, h, j, and i) of OBSs 1–12 and 1–34 for profile GA01 (top row), OBS 2–12 and 2–29 for profile GA02 (middle row) and OBS 3–19 and 3–22 for profile GA03 (bottom row). OBS positions are marked by red dots on top of each profile's model layers. Color scale is identical to Figure 6 and large scale versions of this figure are shown in electronic supplements Figures S1–S6.

divided into two layers with a highly irregular top of the basement which is consistent with the numerous faults and vertical throws identified by Garrocq et al. (2021). Crustal thinning takes place in a ~100 km wide transition zone between the eastern flank of the Aves Ridge and the Grenada Basin. The western flank of the LAA is characterized by a crustal thickness of about 17.5 km, however, the deep central part of the LAA might have not been reached since the easternmost rays are not completely crossing the arc axis. The crust of the eastern margin of the Grenada basin is thinning from 17.5 in the east to 6.5 km in the west over a distance of 45 km. This crustal thickness variation is more abrupt than that across the eastern flank of Aves Ridge. Two distinct crustal layers can be identified along the entire length of the profile and thus under both volcanic arcs, the Aves ridge and the LAA.

3.4.3. Profile GA03

The velocity model for line GA03 is 280 km long and includes 2 sedimentary layers with Vp of 1.9–2.5 km/s and 3.5–3.8 km/s overlying a supra-crustal layer with Vp of 4.5–4.8 km/s, which likely corresponds to volcaniclastic to altered igneous rocks. Overall, these layers thicken in the basin to up to 6–7 km (Figures 11a).

Table 1
Summary of Traveltime Residuals for Each Phases and the Complete Model for Profiles GA01, GA02, and GA03

Phase name	Phase number	Number of picks	RMS error (ms)	Error X^2
GA01 Profil				
Water	1	2524	0.041	0.164
Sediments 1	2	649	0.127	1.624
Sediments 2	3	600	0.143	2.039
Sediments 3	9	193	0.088	0.775
Sediments Reflection 1	4	603	0.073	0.540
Sediments Reflection 2	5	912	0.101	1.024
Sediments Reflection 3	10	1153	0.122	1.480
Sediments Reflection 4	14	810	0.161	2.588
Basement	6	6784	0.108	1.163
Crust reflection	12	530	0.123	1.509
Lower crust	11	7889	0.107	1.143
PmP	7	3157	0.128	1.636
Pn	8	59	0.391	2.249
All phases		27306	0.112	1.250
GA02 Profil				
Water	1	1942	0.057	0.320
Sediments 1	2	835	0.149	2.220
Sediments 3	9	1500	0.111	1.230
Sediments 4	13	837	0.108	1.092
Sediments Reflection 1	4	690	0.083	0.683
Sediments Reflection 2	5	580	0.098	0.957
Sediments Reflection 3	10	130	0.088	0.779
Sediments Reflection 4	14	216	0.169	2.855
Basement	6	6044	0.142	2.009
Lower crust	11	4892	0.108	1.170
PmP	7	2467	0.111	1.225
Pn	8	2584	0.117	1.380
All phases		22608	0.118	1.385
GA03 Profil				
Water	1	1348	0.059	0.342
Sediments 1	2	747	0.164	2.677
Sediments 2	3	1156	0.142	2.004
Sediments 3	9	1178	0.139	1.922
Basement	6	5971	0.112	1.251
Crust reflection	12	776	0.109	1.184
Lower crust	11	7958	0.104	1.081
PmP	7	3160	0.126	1.576
Pn	8	878	0.138	1.903
All Phases		23172	0.115	1.324

Note: "Basement" is the Top of the Upper Crust. "PmP" is the reflection on the Moho discontinuity and "Pn" is the refracted phase in the mantle layer

Along the profile the crustal thickness decreases from 23 km in the west to 10–12 km in the east. It is subdivided into two distinct crustal layers, with velocities between 5.3 and 6.5 km/s at the upper layer and 6.2 and 7.4 km/s in the lower layer. Velocities at the top of the lower layer increase from the East to the West. The crustal thickness at the LAA is 18–19 km, which is about 2–3 km less than the crustal thickness modeled in southern Guadeloupe (Kopp et al., 2011). Although this profile crosses the present active LAA to the outer forearc basin, no reflections from the subducting oceanic crust could be identified.

3.5. Comparison With MCS Data Sections

The supra-crustal part of the wide-angle seismic velocity models presented here are closely consistent with the interpretation of coincident MCS lines GA01 (Figure 12c) and GA02 (Figure 12e) for the corresponding WAS profile, and MCS line GA06 for the western half of GA03 WAS profile (Figures 12a and 13a) (Garrocq et al., 2021). For the eastern part of the GA03 WAS profile, line 2B of the SISMANTILLES 1 cruise was used (Hirn, 2001) (Figure 12b). Three velocity layers, 1.8–2.2 km/s, 2.6–2.7 km/s, and 3.3–3.5 km/s correspond to finely layered seismic units in the basin and the ridge flanks interpreted as sedimentary layers. Underneath, higher velocities 4.5–5.5 km/s (green layer) correspond to low-frequency locally discontinuous layered reflectors supporting a possibly metamorphosed volcano-sedimentary to volcaniclastic rocks nature for this layer, at the bottom of the Grenada Basin in GA02 (Figures 12e and 13c). However, locally, at the Aves Ridge flank, which at least partly emerged in the past, this 1–2-s-twt-thick high-velocity layer is poorly layered and thus also possibly corresponds with an old carbonate platform. Small-scale variations in layers geometry in MCS data are unresolved with the lower-resolution wide-angle approach. Moreover, at least a part of the misfit between wide-angle model GA03 and MCS line 2B of the Sismantilles 1 is likely related to the slight offset between the lines locations. Finally, local discrepancies between MCS interpretation and wide-angle-derived velocity, like the shallow basement associated with relatively low velocities at the top of the Aves Ridge, suggest lateral variations in rock faulting and alteration. Notwithstanding these small-scale discrepancies, the fit between MCS and velocity models derived from wide-angle data is very good.

3.6. Gravity Modeling

We estimate average rocks density from the velocity models and calculate predicted free-air gravity anomalies to be compared to shipboard free-air gravity measurements and thereby confirm the velocity model and allow to extend them into regions unconstrained by seismic rays. Along all seismic profiles, gravity data were acquired using a KSS32M gravimeter from Bodenseewerk. These shipboard gravity data were subsequently corrected for time drift using absolute gravity measurements before and after the cruise and manually cleaned from outliers. In order to reduce high-frequency noise a sliding mean filter and finally the Eötvös correction was applied to these data.

The velocity to density conversion was undertaken using the "Gravmod" software (Zelt & Smith, 1992) which includes a fourth-order polynomial

fit to the relationship of Ludwig et al. (1970; Figure 14). The velocity models were extended by 100 km laterally and to a depth of 110 km to eliminate edge effects. We set the mantle density to a constant 3.32 g/cm^3 (Hotta, 1979), as the information on mantle velocities is scarce in the models and to avoid errors resulting from this. The velocity models are constrained to the depth of the upper mantle only. Therefore, a linear trend has been subtracted from the gravity data to account for a regional signal perhaps related to deeper mantle structure. Mean-root-square errors of the fit between the data corrected for this trend and the predicted anomaly are given in Figure 14.

The predicted free-air gravity anomalies fit the shipboard measurements generally well. Thus, the gravity modeling supports large-scale structures depicted in the velocity models. Also, this modeling allows extending structural interpretations to regions otherwise unconstrained by seismic rays.

Free-air gravity anomalies along the three profiles display variations in three main domains, from west to east. To the west, on the Aves Ridge, the anomalies are positive and increase from ~0 mGal in the north to ~50 to 100 mGal in the south; in the Grenada Basin, the values decrease from north to south, with anomalies between −10 and −30 mGal; and on the LAA, the anomalies are generally positive, between 0 and 100 mGal. A different domain corresponds to the easternmost 50 km of the profile GA03, where the anomalies are negative and they could be associated with the thinner forearc crust above the subduction zone.

The GA03 profile shows a gentle mantle rise from a depth of 27 km in the west to 20 km in the east (Figure 14a). The density in the lower crust changes slightly, from 2.84 to 2.85 g/cm^3; in the upper crust, it goes from 2.68 g/cm^3 in the west, decreasing to 2.63 g/cm^3 in the center, and increasing again to 2.70 g/cm^3 to the east. The significant decrease of the upper crustal density near the OBS 20 (km 120 of the profile), consistent with both WAS and MCS velocities, is possibly related to fracturing in the Montserrat fault zone. In general, the calculated free-air anomaly fits well the data observed. The largest difference between the calculated and measured gravity anomaly values is recognizable in the eastern part of the profile GA03, between the 0 and 60 km model distance, and might be due to the influence of the descending cold slab, which is not imaged by the seismic data and/or non-isostatic anomalies related to active tectonic at the subduction zone and can therefore be not taken into account by the seismic and consequently the gravity modeling.

Along the GA01 profile a significant elevation of the mantle from 27 to 16.5 km from north to south can be observed (Figure 14b). At the lower crustal level, the density change is smooth, from 2.82 to 2.91 g/cm^3; the density of the upper crust remains homogeneous throughout the profile at 2.71 g/cm^3. Compared to the other profiles, GA01 shows the smallest variations in gravity anomaly and also the closest match between the predicted and measured anomalies.

The GA02 profile displays an elongated bell-shaped geometry of the mantle (Figure 14c). From west to east: along Aves Ridge, the Moho depth is 27 km, in the central part of the profile, the Moho depth is 16.5 km, and toward the LAA the top of the mantle is at 21 km of depth. There is only a small density variation in the lower crust, from 2.83 g/cm^3 in the east increasing to 2.85 g/cm^3 toward the central part, and decreasing eastwards to 2.82 g/cm^3 at the LAA. The upper crust remains homogeneous throughout the profile at 2.71 g/cm^3 and the calculated free air anomaly shows a good fit with the observed free-air anomaly.

4. Discussion

Wide-angle seismic models allow constraining the geometry of the sedimentary and crustal layers as well as the nature of the crust by comparison to geological units known from direct sampling. In the following paragraphs, we will compare the results for Aves Ridge and the LAA with other arcs, compare the structure of the margins of the Grenada Basin with other margin types and lastly the oceanic crust and its extent to other oceanic regions.

4.1. Nature of the Crust in the Study Region

In order to identify the nature of the crust along the three profiles, velocity-density profiles were extracted underneath the basement along each profile at an interval of 10 km (Figures 9b–9e, 10b–10e, 11b–11d, and

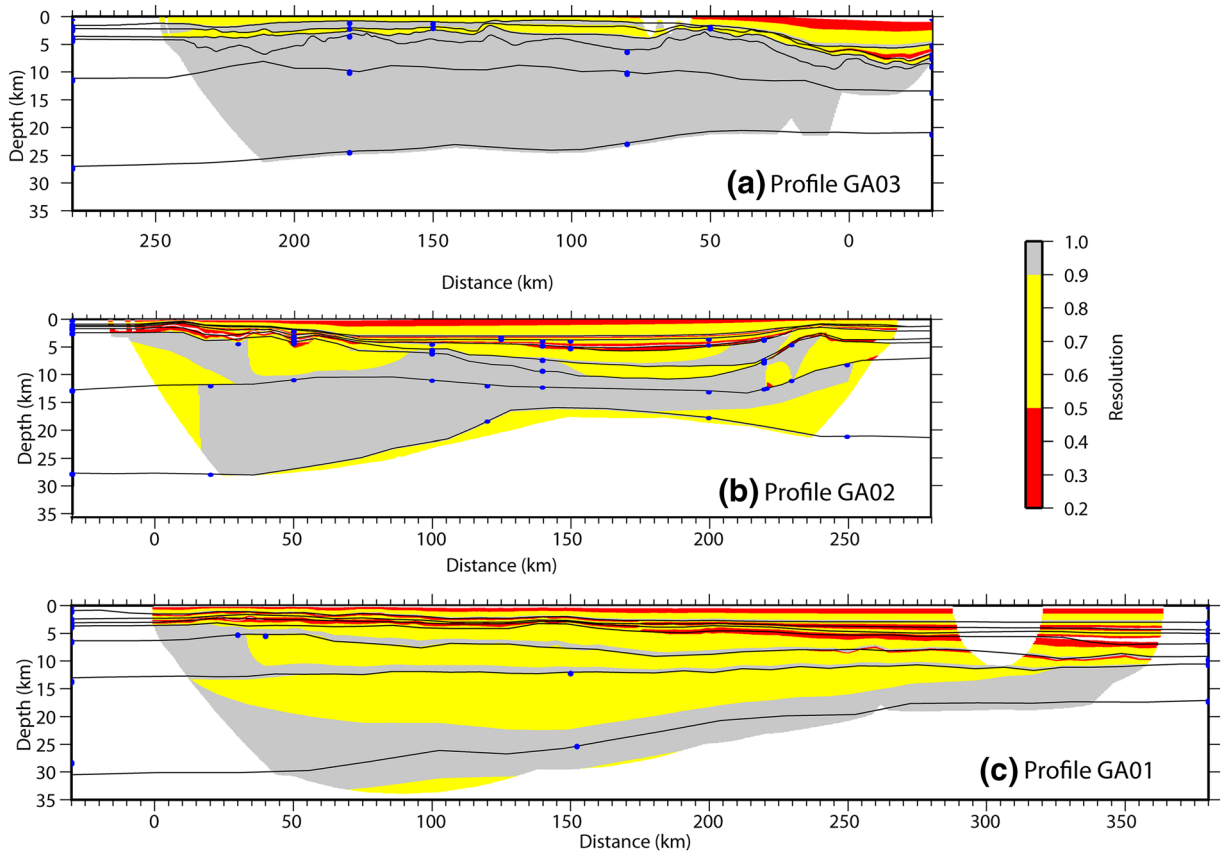

Figure 8. Error estimation of velocity model along of the three profiles. (a) GA03, (b) GA02, and (c) GA01. Model parameterization including interface depth, top and bottom layer velocity nodes (blue circles) and) resolution of velocity (gridded and colored).

15) and then compared to typical oceanic crust (R. S. White et al., 1992), exhumed upper mantle (Dean & Minshull, 2000; Van Avendonk et al., 2006), thinned continental crust (Christensen & Mooney, 1995), typical arc-crust (Kodaira et al., 2007; Shillington et al., 2004) and oceanic plateau crust for example, Cocos Malpelo (Sallarès et al., 2003), and Kerguelen (Charvis et al., 1995). A mean velocity profile was calculated in regions with small changes in crustal thickness. Regions with high lateral changes in crustal thickness are plotted as individual vz-profiles (Figures 9–11).

Best fitting to oceanic crust are GA02 at model distance 120–200 km (Figure 10d) and GA01 at model distance 260–350 km (Figure 9e). The fact that the crust in this region is divided into two layers and up to 10 km thick rule out the possibility of the existence of exhumed and serpentinized upper mantle, as serpentinization only affects the upper 5 km of the crust and in these regions no or only weak reflections from the serpentinization front are detected (Dean et al., 2008). The extent of oceanic crust is about 80 km along GA02 and possibly about 100 km along GA01.

Crust of the Aves Ridge is sampled along the western extremity of profile GA02 (Figures 10b and 15), where it shows a thickness of 25–27 km, which is comparable to other arc-type crust and crust of oceanic plateaus, for example, Izu Bonin and Aleutians (Kodaira et al., 2007; Shillington et al., 2004). A 5–10 km thinner crust can be explained by the fact that the profiles do not sample the thickest part of the ridge or that the arc active life span was shorter. The lower crustal velocities of these arcs are significantly higher than those of average thinned continental crust from Christensen and Mooney (1995; Figure 15). The thicker Izu-Bonin and Aleutian arcs are also characterized by high lower crustal velocities. While these do not exceed 7.2 km/s in the Antilles, velocities of up to 7.7 and 7.6 km/s are found in the Aleutian and Izu-Bonin arc respectively. As has been proposed earlier, these differences might be explained by a thick layer of mafic and ultra-mafic cumulates at the base of the crust of the Izu-Bonin and Aleutian arc, which is smaller or missing in the Antilles (Christeson et al., 2008) and in good agreement with the

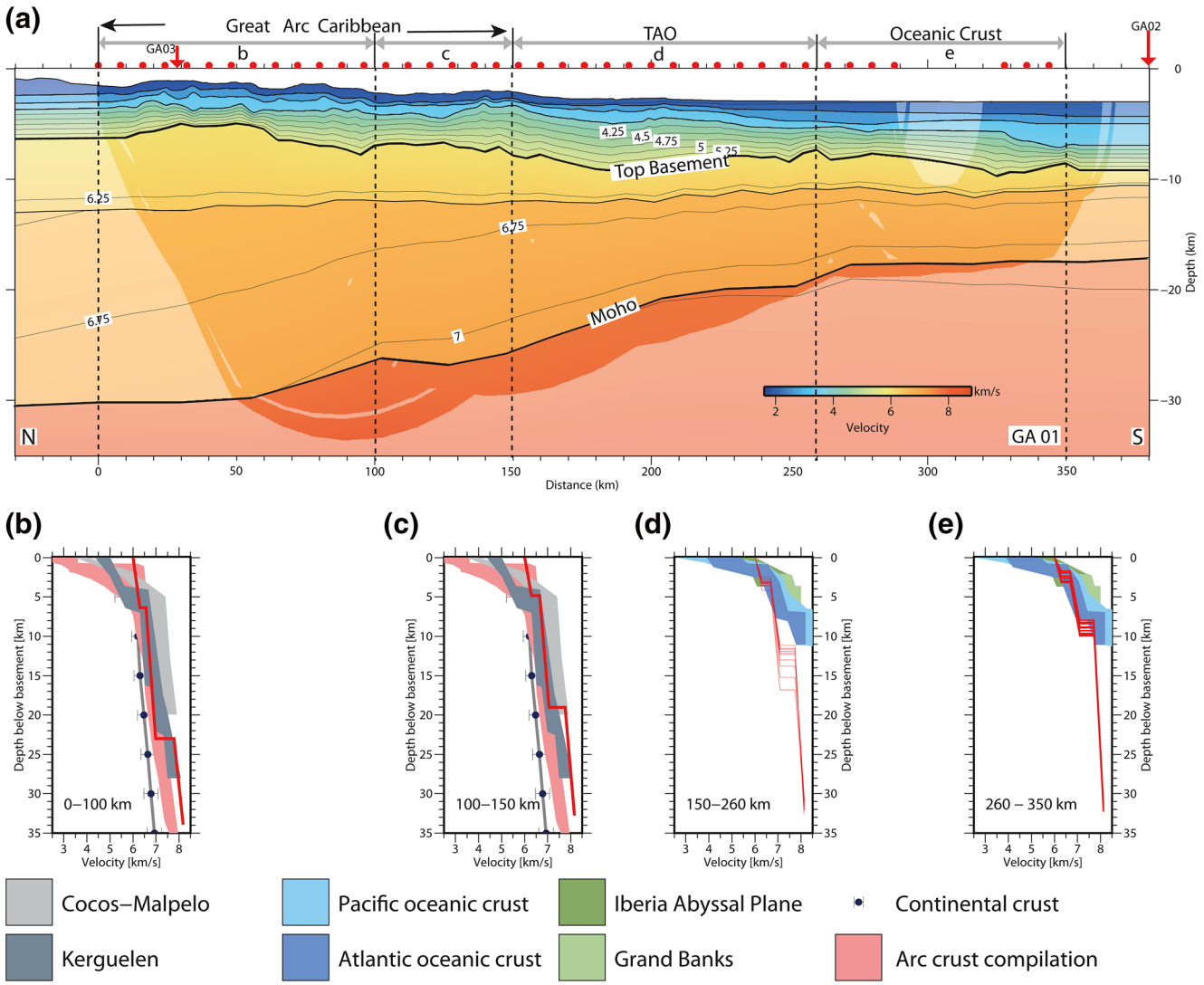

Figure 9. (a) Final velocity model of GA01 contoured every 0.25 km/s. Bold black lines represent layer boundaries. (b) Mean vz-profile from the region between 0 and 100 km model distance and comparison to thinned continental crust with black dots (Christensen & Mooney, 1995), Cocos Malpelo (Sallarès et al., 2003), and Kerguelen (Charvis et al., 1995). Red envelope marks outline of arc crusts detailed in Figure 15. (c) Mean vz-profile from the region between 100 and 150 km model distance and comparison to thinned continental crust, Cocos Malpelo (Sallarès et al., 2003), and Kerguelen (Charvis et al., 1995). (d) Vz-profiles from the region between 150 and 260 km model distance and comparison to typical oceanic crust from the Atlantic and Pacific (R. S. White et al., 1992) and serpentinized upper mantle (Dean et al., 2008; Van Avendonk et al., 2006). (e) Vz-profiles from the region between 260 and 350 km model distance and comparison to typical oceanic crust from the Atlantic and Pacific and serpentinized upper mantle. GA, Great arc of the Caribbean; TAO, Transition Arc-Ocean.

lower production rate in the Antilles (Wadge, 1984). We cannot exclude an oceanic plateau origin since the seismic velocities are compatible with thickened oceanic crust. The arc-ocean transition zone sampled in profiles GA01 and GA02 (Figures 9d and 10c) shows gradients and velocities highly similar to those of the Aves Ridge and thus probably indicating a volcanic origin. Crustal thinning takes place in a ~100 km wide transition zone along GA02 between the eastern flank of the Aves Ridge and the oceanic part of the Grenada Basin.

The crust of the LAA region is sampled by GA03 between 50 and 200 km, with a transition on both sides, toward the Aves Ridge and the forearc domain (Figures 11c), and GA02 between 200 and 280 km (Figure 10e). It has very similar characteristics to Aves Ridge, however its thickness does not exceed 25 km, which is in good agreement with earlier wide-angle seismic studies (C. B. Officer et al., 1957; Boynton et al., 1979; Kopp et al., 2011), petrology of crustal xenoliths and seismic receiver functions (Melekhova et al., 2019) and receiver function studies (Gonzalez et al., 2018; Schlaphorst et al., 2018; Sevilla et al., 2010), which show

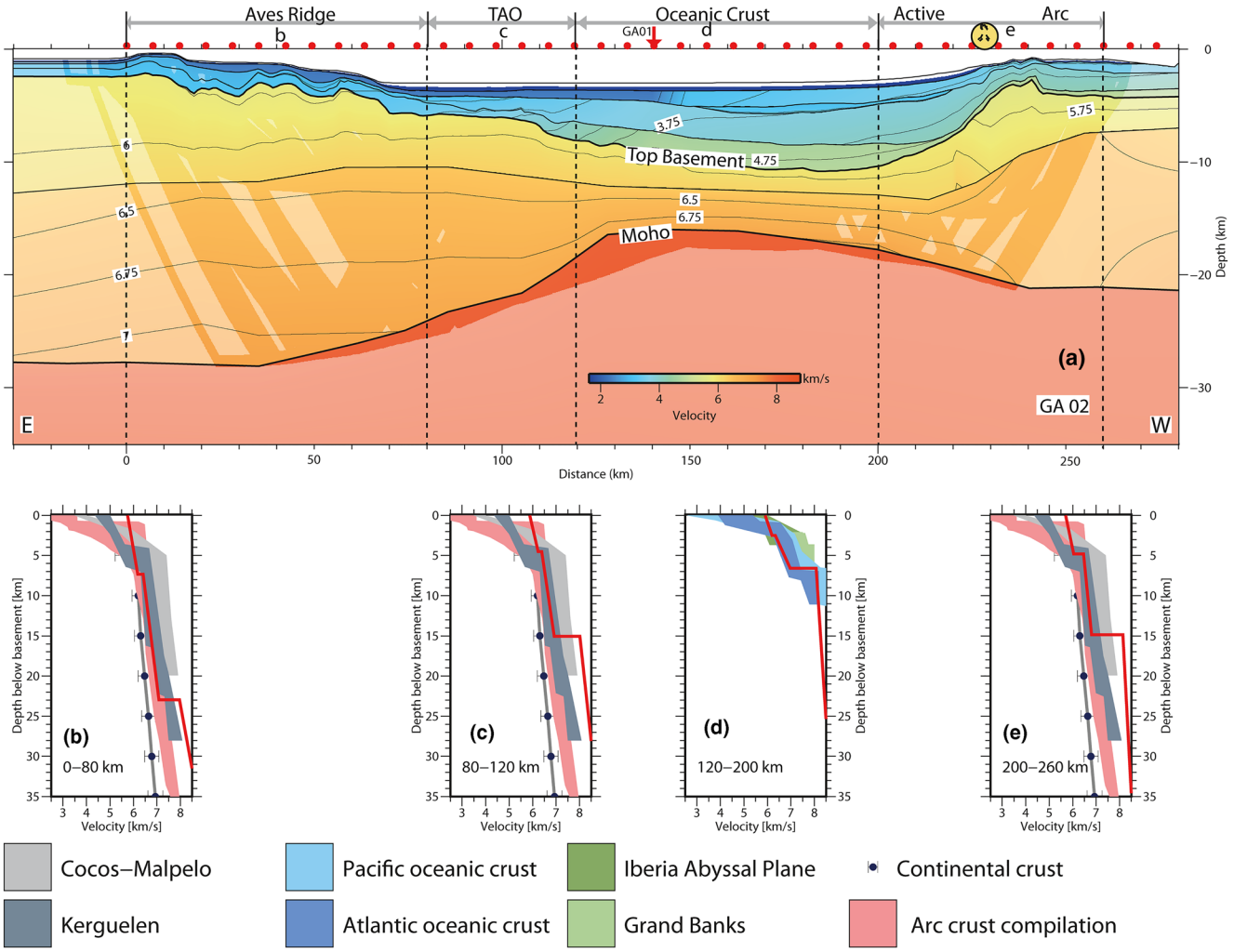

Figure 10. (a) Final velocity model of GA02 contoured every 0.25 km/s. Bold black lines represent layer boundaries. (b) Mean vz-profile from the region between 0 and 80 km model distance and comparison to thinned continental crust (Christensen & Mooney, 1995), Cocos Malpelo (Sallarès et al., 2003), and Kerguelen (Charvis et al., 1995). Red envelope marks outline of arc crusts detailed in Figure 15. (c) Mean vz-profile from the region between 80 and 120 km model distance and comparison to thinned continental crust, Cocos Malpelo (Sallarès et al., 2003), and Kerguelen (Charvis et al., 1995). (d) Vz-profiles from the region between 120 and 200 km model distance and comparison to typical oceanic crust from the Atlantic and Pacific (R. S. White et al., 1992) and serpentinized upper mantle (Dean et al., 2008; Van Avendonk et al., 2006). (e) Vz-profiles from the region between 200 and 280 km model distance and comparison to thinned continental crust (Christensen & Mooney, 1995), Cocos Malpelo (Sallarès et al., 2003), and Kerguelen (Charvis et al., 1995). TAO, Transition Arc-Ocean.

variable thicknesses between 25 and 35 km thick crust along the active arc. The velocity-depth curves from the Aves Ridge and the LAA and forearc region show that seismic velocities in both structures are similar (Figure 15) indicating that the composition of rocks might be similar in both regions. In the assumption that the absence of significant differences might indicate a similar origin of arc-type crust, small differences in velocity might be due to local inhomogeneities or due to cooling of the remnant Aves Ridge as proposed in earlier studies (Christeson et al., 2008; Clark et al., 2008). An origin from thickened oceanic crust heavily intruded by volcanism cannot be excluded.

The integration of 1D velocity-depth curves extracted along the three OBS profiles with the profiles published by Christeson et al. (2008) and Kopp et al. (2011) allows proposing a schematic distribution of the nature of the crust in the study area (Figure 16). The spatial distribution of the different 1D velocity-depth profiles indicates the existence of several regions underlain by crust of differing nature. Arc-type crusts are interpreted along both the Aves Ridge and the LAA domain, which velocity structure and thickness only differ slightly, probably due to their different evolution. In the south-west Grenada Basin,

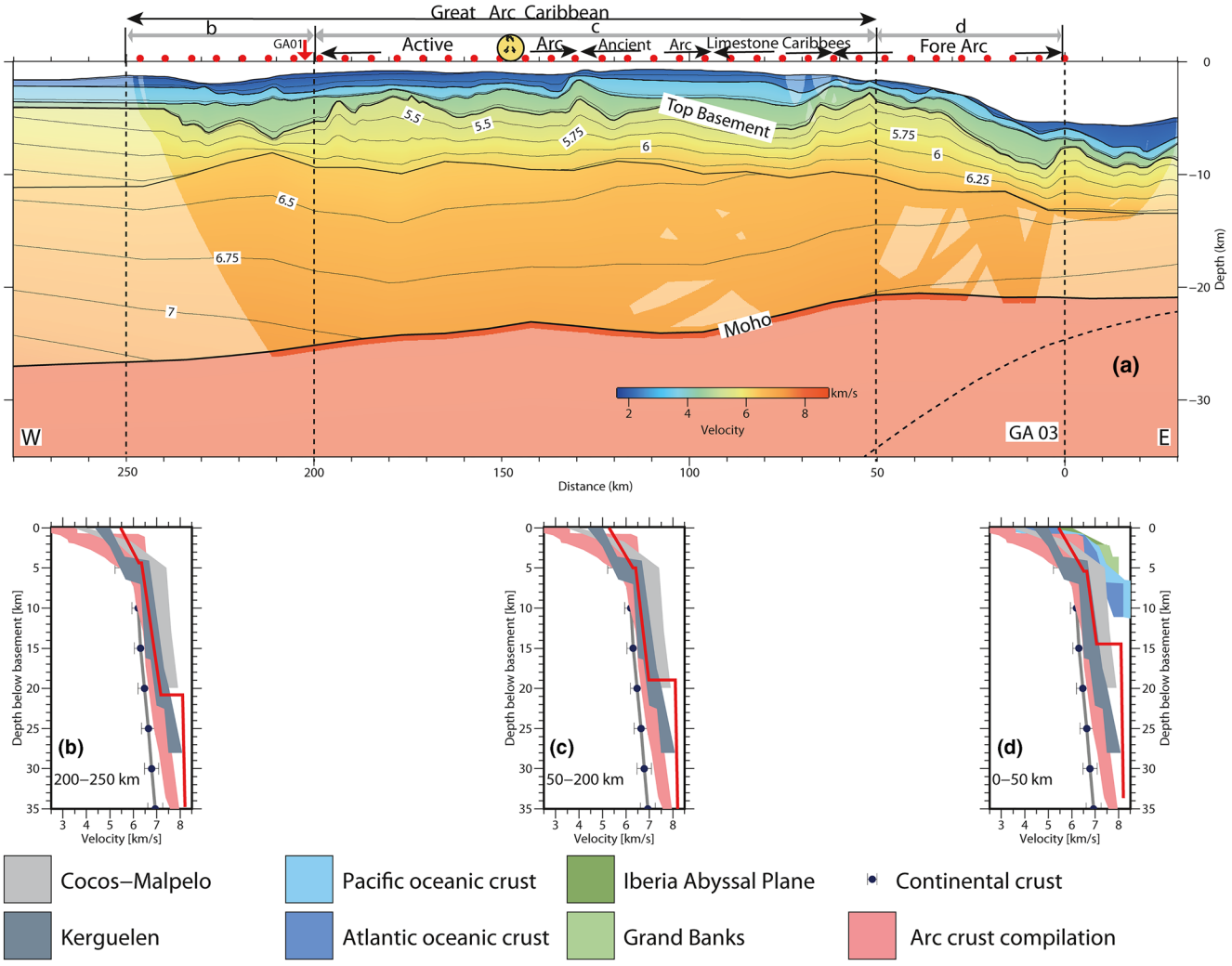

Figure 11. (a) Final velocity model of GA03 contoured every 0.25 km/s. Bold black lines represent layer boundaries. The dotted black line outlines the expected position of the downgoing plate roof as extrapolated from MCS data in the area (Laigle et al., 2013). (b) Mean vz-profile from the region between 200 and 250 km model distance and comparison to thinned continental crust (Christensen & Mooney, 1995), Cocos Malpelo (Sallarès et al., 2003), and Kerguelen (Charvis et al., 1995). Red envelope marks outline of arc crusts detailed in Figure 15. (c) Mean vz-profile from the region between 50 and 200 km model distance and comparison to thinned continental crust, Cocos Malpelo (Sallarès et al., 2003), and Kerguelen (Charvis et al., 1995). (d) Vz-profiles from the region between 0 and 50 km model distance and comparison to typical oceanic crust from the Atlantic and Pacific (R. S. White et al., 1992) and serpentinized upper mantle (Dean et al., 2008; Van Avendonk et al., 2006). GA = Great arc of the Caribbean.

the velocity structure corresponds to an oceanic crust. These main domains are separated by transitional zones of unknown or mixed crustal type between the remnant Great Arc of the Caribbean in the west and the LAA domain in the east and the oceanic crust in the southern part of the study region. In the northern part, the transition zone is sandwiched between Aves Ridge and the highly curved LAA in the north.

4.2. Comparison of the Grenada Basin Margins With Other Continental Margins

The comparison to other rifted and transform margins allows to draw conclusions about the opening and formation of the Grenada Basin (Figure 17). The width of the transition zone yields information about opening processes and the amount of volcanic products at the margin allows constraining the thermal state of the rift. In the following paragraphs, the Grenada basin structure will be compared to rifted magma-poor and magmatic margins as well as to transform margins from other regions.

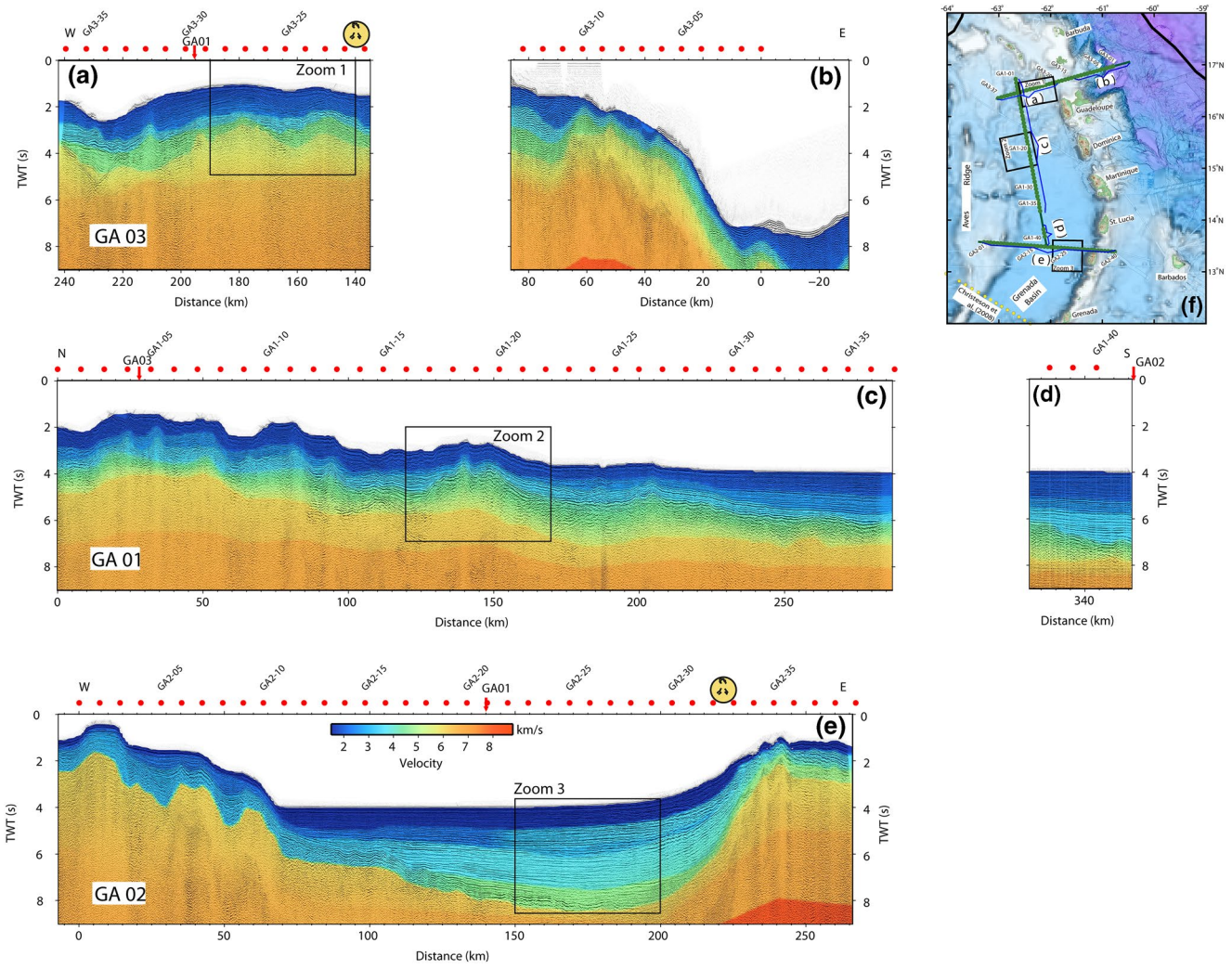

Figure 12. Reflection seismic sections from the Garanti and Sismantilles 1 cruise (Hirn, 2001) with velocities from wide-angle seismic models underlain. (a) Garanti MCS profile 6 underlain by GA03 WA model. (b) Sismantilles 1 MCS profile 2B underlain by part of GA03 WA model. (c) Garanti MCS profile 3–2 underlain by part of GA01 WA model. (d) Garanti MCS profile 3–1 underlain by part of GA01 WA model. (e) Garanti MCS profile 2 underlain by part of GA02 WA model. (f) position of MCS and the wide-angle profiles. Black boxes show the position of the zooms presented in Figure 13.

Magma-poor rifted margins, such as the conjugate Nova Scotia and Moroccan margin are usually asymmetrical with typically 50–150 km wide ocean-continent transition zones bounding a 100–300-km-wide zone of thinned continental crust (Figures 17f and 17g) (Biari et al., 2015; Funck et al., 2004). The comparison of profile GA02 to these two rifted Atlantic margins indicates that lower crustal velocities are lower with also a lower velocity gradient at the Atlantic margins than along Aves Ridge and the active LAA (Figures 17d, 17f, and 17g). Between clear continental and oceanic crust along magma-poor continental margins, a region of exhumed serpentinized upper mantle material is imaged (Figure 17f) (e.g., Funck et al., 2004; Sallarès et al., 2013). It is proposed to be linked to the low rate of volcanic production before the onset of mantle upwelling and melting leading to oceanic crustal accretion (Jagoutz et al., 2007; Klingelhoefer et al., 2014). The first oceanic crust produced after breakup can be variable and atypical, and very thin (2–3 km) (e.g., Funck et al., 2004; Wu et al., 2006). In comparison, the margins of the Grenada Basin along profile GA02 are only 50–80 km wide and no zone of serpentinized upper mantle material was detected in the transition zone by this study. The oceanic crust is uniformly 7–8 km thick, typical for normal oceanic crust (R. S. White et al., 1992). The absence of thin oceanic crust and elevated lower crustal velocities of the Grenada Basin as compared to magma-poor rifted margins indicates that opening here was accompanied by elevated mantle temperatures.

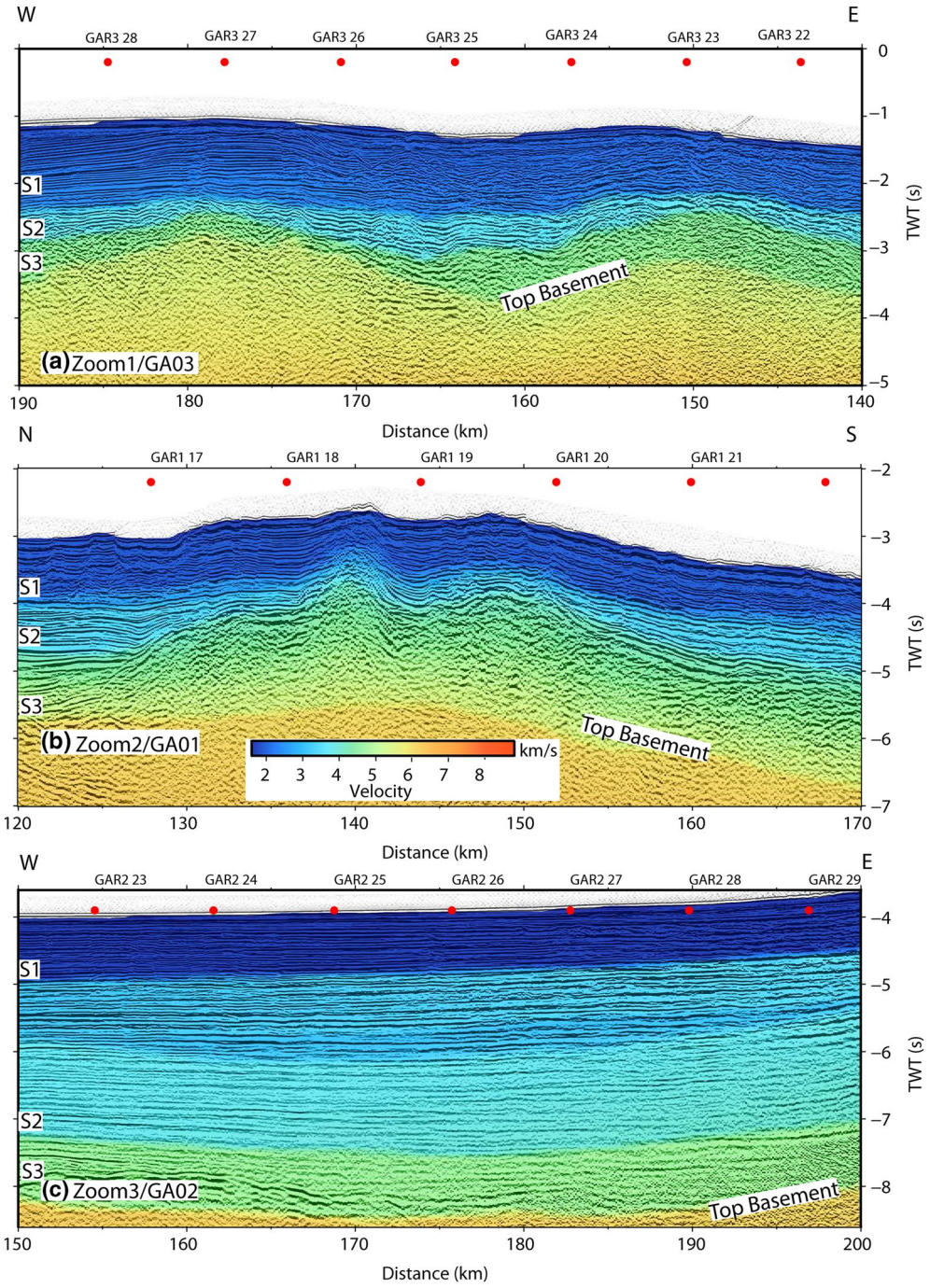

Figure 13. Zoom 1, 2, and 3 from of the wide-angle seismic velocity models consistent with the interpretation of MCS. (a) Zoom 1 profil GA03, (b) zoom 2 profil GA01; and (c) zoom 3 profil GA02. S1, sedimentary layer 1; S2, sedimentary layer 2; S3, sedimentary layer 3.

If rifting is accompanied by elevated potential mantle temperatures, the rifting and opening of the margin will be characterized by an abundance of volcanic products in form of seaward dipping reflectors and magmatic underplating (e.g., the Argentine margin [Franke et al., 2010]) and the Greenland margin (Holbrook et al., 2001). At these types of magmatic margins, the first oceanic crust can be up to 10–15 km, therefore significantly thicker than typical oceanic crust of 6–7 km thickness (Christeson et al., 2019; Van Avendonk et al., 2017; R. S. White et al., 1992) (e.g., the magmatic Namibian margin [Bauer et al., 2000]) and US continental margin (LASE Study Group, 1986).

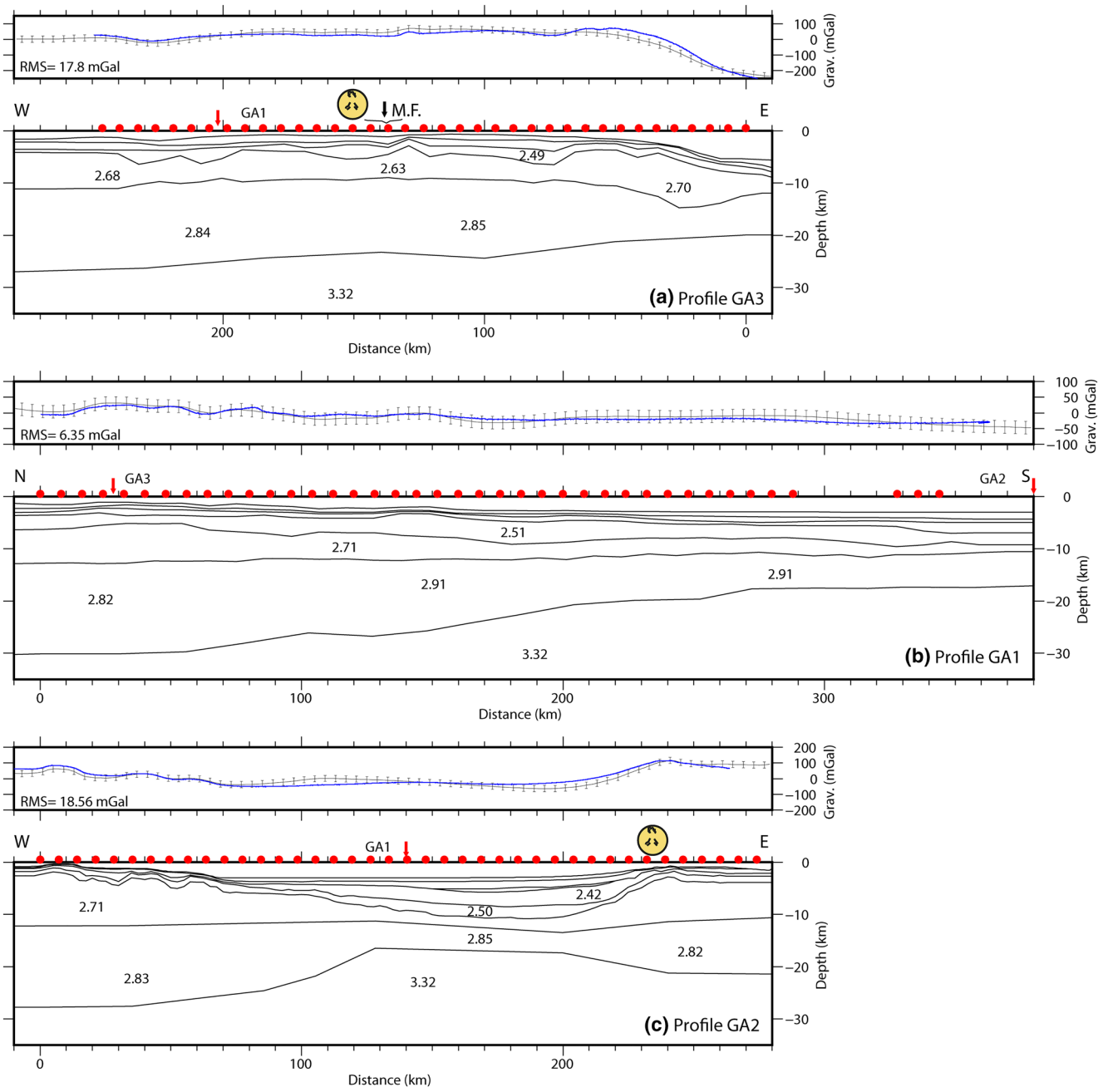

Figure 14. Results of the gravity modeling along the three transects. Italic numbers give the densities used in the model, red dots mark positions of the instruments, and arrows the crossings with other profiles. Black Arrow (M.F.) Montserrat Fault. Blue lines are the predicted gravity free-air anomaly from modeling and black lines the shipboard measured free-air gravity anomaly with 20 mGal error bars.

Although no underplating or thickened oceanic crust has been imaged in the Grenada Basin, moderate volcanism accompanied the opening of the basin. Thus, the opening was accompanied by a lower degree of mantle melting and probably a lower potential mantle temperature than typical volcanic margins leading to the accretion of normal thickness oceanic crust in the Grenada Basin. This study clearly indicates a moderate influence of volcanism during opening of the basin.

Transform or highly oblique margins are characterized by a narrow continent-ocean transition zone (Basile et al., 1996; Mascle & Blarez, 1987). The NE Algerian margin is proposed to have opened as a highly oblique or transform margin (Badji et al., 2015; Klingelhoefer et al., 2015) (Figure 17e). The continent-ocean

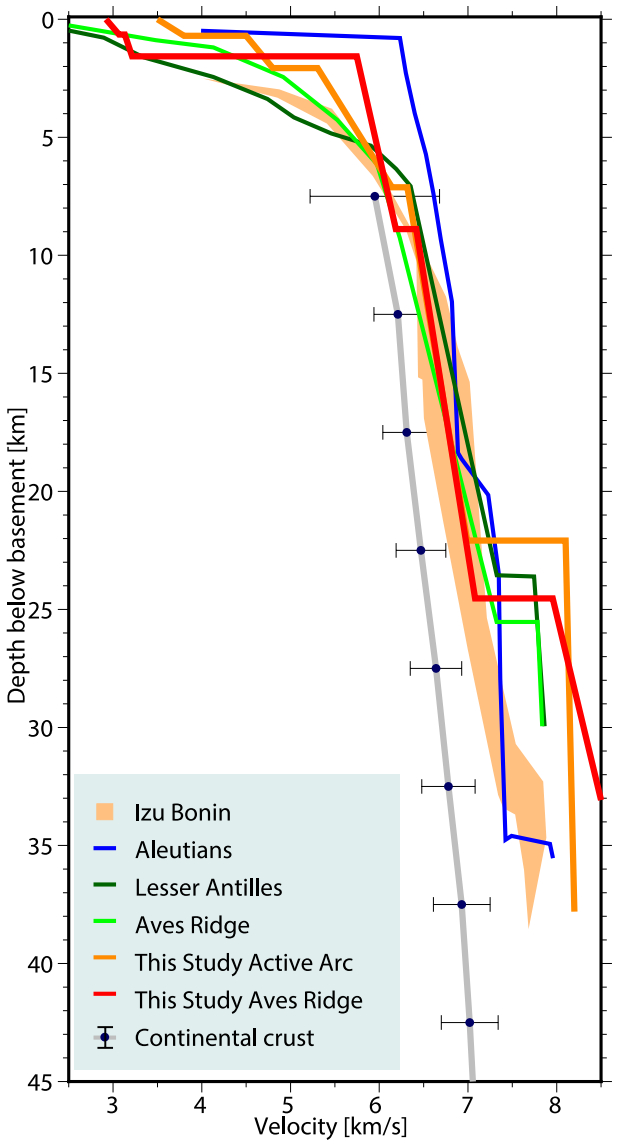

Figure 15. Comparison of velocity-depth relationship underneath the seafloor for Aves Ridge (red line) and the Lesser Antilles modern arc (orange line) from this study to Izu Bonin (orange polygon [Kodaira et al., 2007]) and Aleutian arcs (blue line [Shillington et al., 2004]). Also shown are a velocity-depth relationship from Aves Ridge (green line [Christeson et al., 2008]) and the Lesser Antilles modern arc (dark green line [Kopp et al., 2011]) and thinned continental crust with a 2.5 km thick sedimentary layer added for comparison (Gray line [Christensen & Mooney, 1995]).

transition zone is only 30 km wide thinning from 26 km to only 5 km crustal thickness. The seismic velocities of the north Algerian margin are typical for continental crust and the oceanic crust is thinner than typical Atlantic oceanic crust. Volcanic products are rare in the region. A second example of transform or highly oblique opening is the Demerara Plateau in the Equatorial Atlantic (Figure 17c). Here opening was accompanied by heavy volcanism leading to the deposition of large amounts of seaward dipping reflector (SDR) packages building a large part of the plateau (Museur et al., 2020; Reuber et al., 2016). Some volcanic edifices are identified in our study region (Garrocq et al., 2021) and the sedimentary sequences might contain volcano-sedimentary layers. Although dipping reflections identified in the MCS data are interpreted to correspond to lava flows, these do not have the same thickness as the SDR commonly identified along volcanic margins or at transform margin plateaus such as the Demerara plateau where they can reach a thickness of up to 21 km (Reuber et al., 2016). Comparing these two margins to the Grenada Basin indicates that the narrow transition zone in our study region might result from transform or highly oblique rifting, however the amount of volcanism corresponds to neither of the two comparison margins.

A third possible comparison is that to other back-arc basins, as for example, the Liguro-Provencal Basin (Afilhado et al., 2015; Gailler et al., 2009; Moulin et al., 2015) which opened as a back-arc basin between the Gulf of Lions and West Sardinia through rotation of the Corso-Sarde block (Figures 17a and 17b). The resulting margins show a clear asymmetry in the TOC and are marked by zones of high lower crustal velocities with velocities comparable to the serpentinized upper mantle material sampled along Atlantic margins. These zones are bordering thin oceanic crust. No such zones have been imaged in the Grenada basin. Although the Sardinian margin shows rapid thinning, the conjugate Gulf of Lions margin shows a 150–200 km wide zone of crustal thinning comparable to an Atlantic margin (Figures 17a–17b and 17f–17g). This comparison shows that the width and structure of the transition zone are not only the direct result of rifting in a back-arc environment.

As a conclusion, these comparisons indicate that opening of the Grenada Basin might have occurred in a transform or highly oblique direction, at least in the south, and was accompanied by a moderate quantity of volcanism. The fact that normal oceanic crust was accreting in the southern part of the basin excludes the existence of a large mantle thermal anomaly or hotspot at the origin of the breakup, as this would have led to the accretion of anomalous thick oceanic crust. However, the thicker, possibly oceanic, crust, and presence of small volcanic edifices in the northern Grenada Basin could attest for the influence of a moderate thermal anomaly.

4.3. Nature, Spreading Direction, and Extent of the Oceanic Crust in the Grenada Basin

Where imaged with seismic data, oceanic crust in the Grenada Basin is of typical thickness (6–8 km) for Atlantic-type oceanic crust as compiled in R. S. White et al. (1992). It is divided into two layers, with the upper layer of about ⅓ of the overall thickness likely corresponding with oceanic layer two pillow basalts and sheeted dykes. The seismic velocities in this layer are slightly elevated compared to oceanic crust close to the accretionary ridges, but this can be explained by the overlying sediment load closing pore spaces and compacting the volcanic products. The underlying layer with velocities between 6.30 and 7.10 km/s is

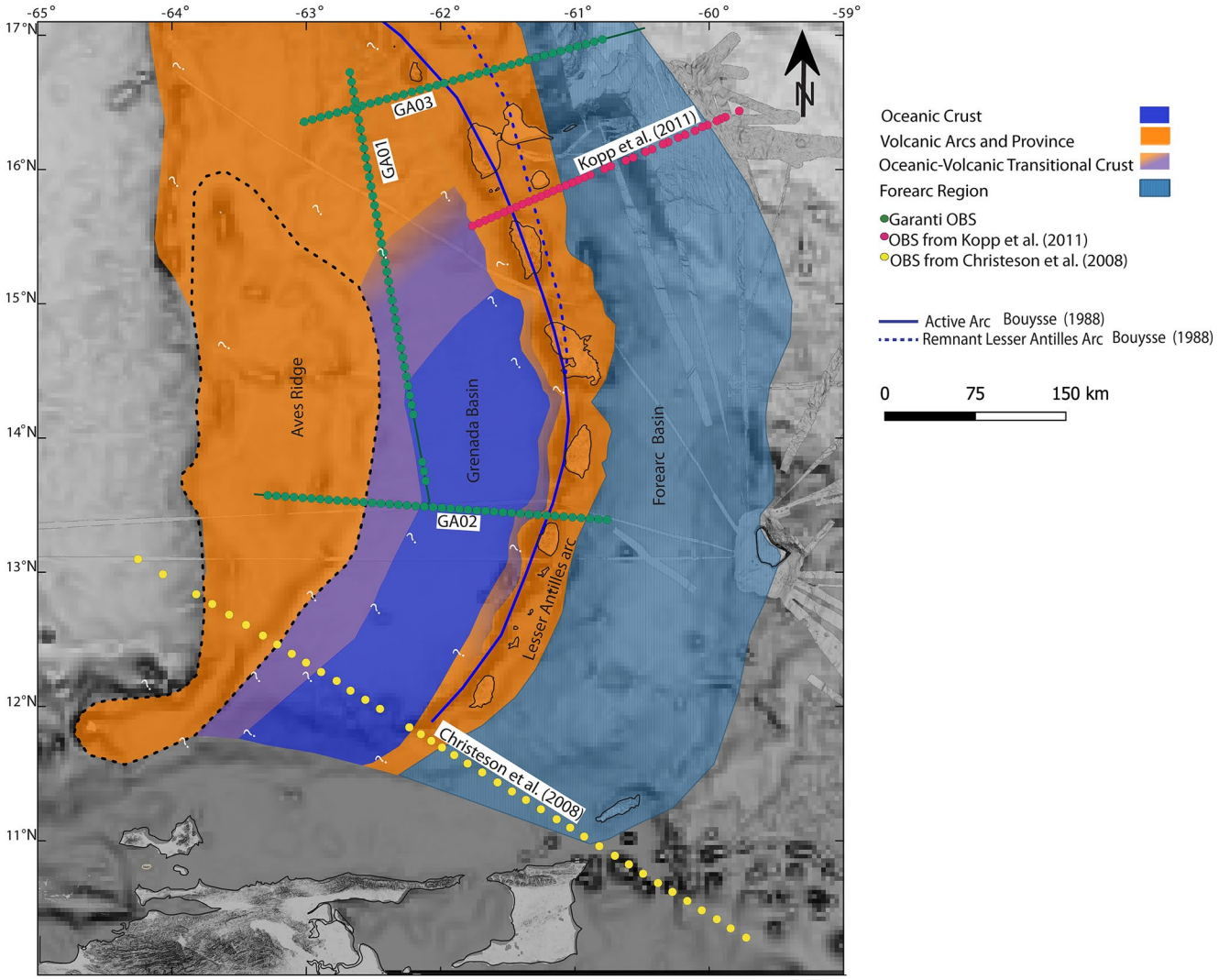

Figure 16. Schematic distribution of crustal nature based on the velocity structure along profiles GA01, GA02 and GA03 (green dotted lines). (1) Thick volcanic crust along the Aves Ridge and the active LAA (orange color); (2) oceanic crust (blue color); (3) Transition zones between the oceanic crust and the thick volcanic crust (diffuse purple to orange color).

likely to correspond with layer three cumulate mafic rocks. At slow or ultra-slow spreading rates, a high amount of exhumed mantle material can be incorporated into the oceanic crust (Cannat et al., 2006; Sauter et al., 2013; Smith, 2013). Slow spreading often forms proto-oceanic crust after first oceanisation of a magma-poor margin leading to regions with oceanic crust with high serpentinite content or exhumed mantle material only close to the margins (Cannat et al., 2009; Jagoutz et al., 2007; Klingelhoefer et al., 2014). However, no such zone is imaged along the oceanic crust in the Grenada Basin as a comparison to regions of exhumed upper mantle at continental margins clearly indicates (Figure 17c vz-panel in the basin and comparison to exhumed upper mantle from the Iberia Abyssal Plain) (Dean et al., 2008) and the Grand Banks (Van Avendonk et al., 2006).

The oceanic crust is restricted to the southern part of the Grenada Basin, inconsistent with tectonic models by Tomblin (1975) and Bird et al. (1999) which both require an extension of the oceanic crust throughout the complete basin, either accreted in an east-west or diffuse way (Figure 2). The Grenada Basin asymmetry might testify of an extension underneath the current location of the active LAA as proposed by Aitken et al. (2011) and Allen et al. (2019). This asymmetry could also be related to a complex opening structured with spreading axes shifted along transform faults (J. L. Pindell and Kennan, 2009). The extent of the oce-

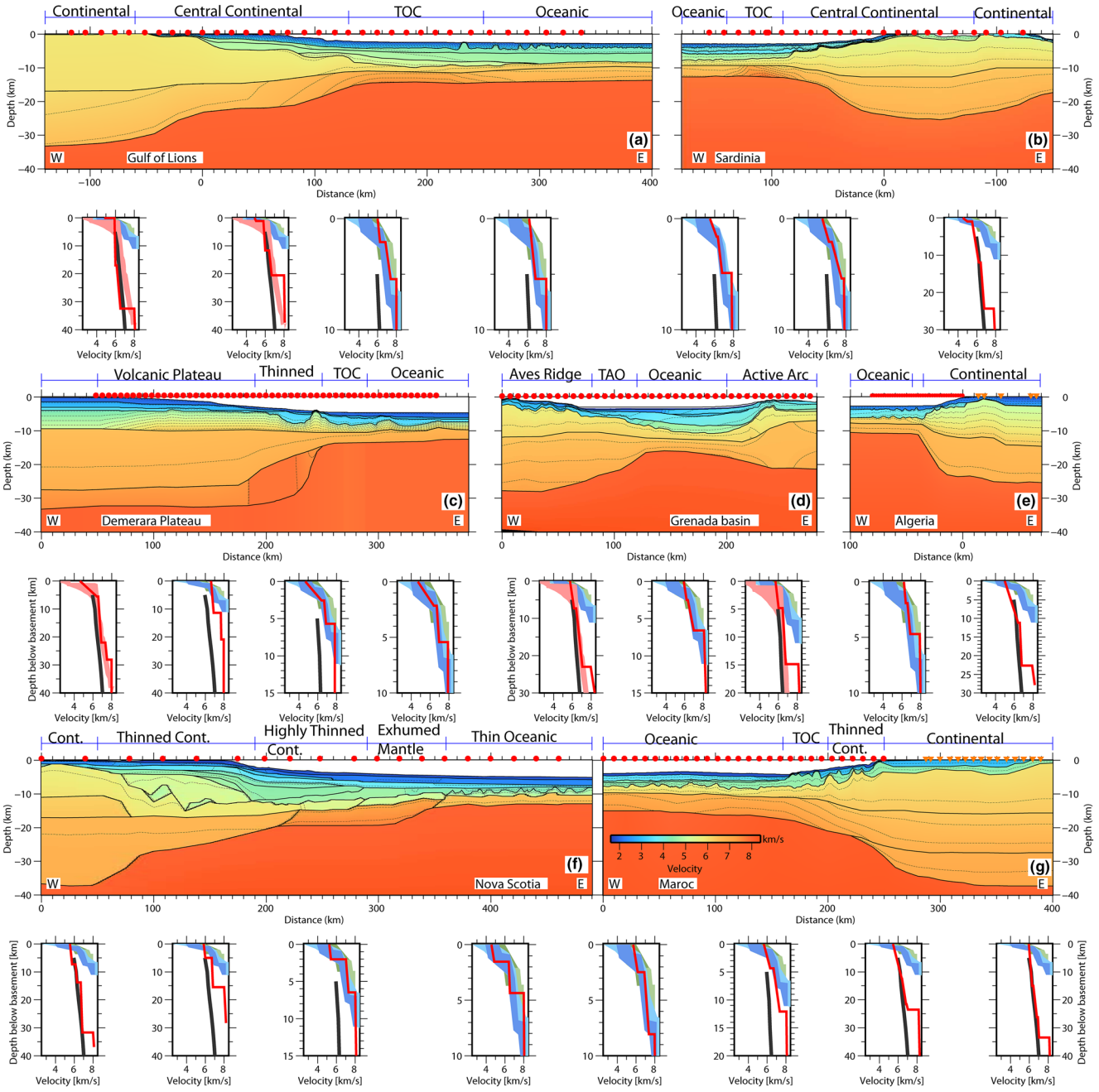

Figure 17. Comparison of the GA02 velocity model with other margins and plateaus: (a) and (b) Liguro-Provencal Basin (Afilhado et al., 2015; Gailler et al., 2009; Moulin et al., 2015); (c) Demerara (Museur et al., 2020); (d) this study; (e) Algeria (Badji et al., 2015; Klingelhoefer et al., 2014); (f) Nova Scotia (Funck et al., 2004); (g) Morocco (Biari et al., 2015). TOC, Transition Ocean-Continent, TAO, Transition Arc-Ocean. (Location map of all profiles is presented in electronic Figure S10).

anic crust over 80 km seems to rule out an origin from a forearc basin, which is generally restricted to the onset of subduction (Kodaira et al., 2010).

The Aves ridge has been proposed to be the Paleocene remnant volcanic arc of a westward subduction (e.g., Tomblin, 1975). However, the deeper crust of the ridge has not been sampled by scientific drilling, and velocities from wide-angle seismic studies do not allow to discriminate between an origin from volcanic arc crust or oceanic plateau crust. Along the eastern border of the basin, the LAA has been imaged by wide-angle seismic data and here an origin of the arc from volcanic products intruding a thick plateau crust

has been proposed (Evain et al., 2013; Kopp et al., 2011; Laigle et al., 2013). The fact that along the northern profile GA03 the crust is characterized by a nearly constant crustal thickness and displays only small velocity variations from Aves ridge to the LAA might indicate a common origin for the crust of both arcs. Furthermore, it seems unlikely that these large volumes of crust can have been produced by the otherwise scarce Antilles volcanism. An alternative interpretation, therefore, is that both crustal bodies (Aves Ridge and LAA) were formed by volcanic intrusions into existing thick plateau crust, and/or by an older and more vigorous volcanic phase in the northern part of the basin (north of Martinique island). This intruded oceanic plateau may thus include the entire northern region from the Aves Ridge to the active and ancient arcs and the southern LAA basement but further investigations are required to verify this.

Many back-arc basins are characterized by thin oceanic crust, such as the Lau basin (~4 km) (Crawford et al., 2003), the Philippine Sea and Parece Vela Basin (~3–4 km) (Louden, 1980), the western Mediterranean basins (~4 km) (e.g., Gulf of Lions: Afilhado et al., 2015; Moulin et al., 2015), and the Algerian Basin (~5.5 km): Aïdi et al., 2018; Leprêtre et al., 2013). This thin crust has been proposed to result from unusually low mantle temperatures due to the subduction of a cold slab, for example, in the Philippine Sea basin (Louden, 1980; Sclater et al., 1976) and in the Provençal basin (~4 km) (Gailler et al., 2009). The oceanic crust in the Grenada Basin is of normal thickness and probably to a high extent of magmatic origin, indicating that here the mantle temperatures at the onset of seafloor spreading were not unusually low and possibly even high in the northern part.

Even though most back-arc basins open in the direction of the relative motion of the ongoing plate convergence (Jurdy & Stefanick, 1983), oblique opening back-arc basins are not uncommon with an increasing amount of extension from one side of the arc to the other (Schellart et al., 2002). For example, the Havre Trough, to the rear of the Kermadec arc, is opening by oblique back-arc rifting propagating into the continental margin of New Zealand (Benes & Scott, 1996) and the Okinawa Trough which is currently still in an oblique rifting stage (Sibuet et al., 1987). Oblique extension can also facilitate rifting and break-up requiring less force to reach the plastic yield limit (Brune et al., 2012). Changes in the rifting direction can be linked to the location of slab tear faults (Schellart et al., 2002). Although the Garanti wide-angle seismic data set does not allow to unequivocally constrain the direction of rifting and first spreading in the Grenada basin, we might speculate that the existence of North American–South American boundary in the subducting oceanic plate might have influenced the extent of oceanic crust in the Grenada Basin.

5. Conclusions

Modeling of three wide-angle seismic profiles from the Grenada Basin in the Antilles region between Aves Ridge and the modern arc, combined with reflection seismic profiles and gravity data, have allowed us to interpret the nature of the crust, Moho depth and the structure of the sedimentary infill of the basin in four main domains, from west to east:

1. At the eastern flank of Aves Ridge, the crust is between 25 and 27 km thick and can be divided into two layers. The upper layer is ~7 km thick with velocities between 5.8 and 6.4 km/s and the lower layer about 17 km with velocities between 6.5 and 7.1 km/s. The Aves Ridge free air gravity response is characterized by positive anomalies, which shows an increment from north to south, ranging from near 0 to 100 mGal.
2. In the southern part of the Grenada basin an 80 km wide region of oceanic crust was identified, with a thickness normal for typical oceanic crust of 6–7 km and velocities between 6.0 and 6.7 km/s. The free air gravity anomaly is characterized by negative anomalies ranging from near ~ −10 in the north to −30 mGal in the south.
3. Crustal thinning takes place between the eastern flank of the Aves Ridge and the oceanic part of the Grenada Basin and from the center of the basin toward the north. The crust at the eastern arc-ocean transition zone is thinning from 27 to 8 km over a distance of only 80–100 km. It is characterized by velocity gradients similar to those of the remnant Aves Ridge and thus probably indicating an origin from the volcanic arc. The N-S transition zone is at least 150 km wide, leading to a more gentle change of crustal thickness. As in the E-W transition zone, velocities and velocity gradient indicate the presence of a volcanic arc-type crust or plateau. Here, the free air gravity anomaly is characterized by negative anomalies which decrease further from north to south, ranging from near 0 to −25 mGal.

4. The active LAA crust has very similar characteristics to Aves Ridge with velocities ranging from 5.8–6.8 km/s and a subdivision into two distinct layers. Its free air gravity anomaly is similar to that of Aves Ridge, however, its thickness does not exceed 25 km along our profiles.

The velocity-depth curves from the Aves and active LAA region show that seismic velocities in both structures are similar indicating that the composition of rocks at Aves Ridge is similar to that of the active arc. A comparison of velocity-depth curves from Aves Ridge and the modern arc with other regions shows similarities with other volcanic arcs, such as the Izu-Bonin or Aleutians, characterized by lower crustal velocities higher than in typical thinned continental crust. Similar velocity characteristics are found along volcanic plateaus such as the Demerara Plateau. The width of the E-W arc ocean transition zone is smaller than at Atlantic rifted margins, and resembles those of transform margins, however the N-S volcanic arc basin transition is 150 km wide indicating a more gradual rifting. We propose that the Grenada Basin opened in an oblique way and under influence of moderate volcanism.

Data Availability Statement

The wide-angle seismic data in SEGY format with navigation information in the headers used in this study are available for download at SEANOE: https://doi.org/10.17882/74223. The seismic velocity models are also available for download at SEANOE: https://doi.org/10.17882/76298.

Acknowledgments
The authors would like to thank the captain and the crew of R/V L'Atalante and the technical seismic teams of Genavir and the UMR Géoazur for their excellent work during the data acquisition. Warmest thanks to Alison Chalm for help with the English. The authors would like to thank Gail Christeson and Robert Allen for constructive reviews which helped to improve the manuscript. The authors acknowledge the ANR 17-CE31-0009 GAARANTI project for funding of parts of the marine study, and the PAUSE program and IFREMER for funding Crelia Padron's stay in France. The CNRS-INSU funded travel for the cruise participants and a post-cruize meeting. The GARANTI cruise team includes Jean-Frédéric Lebrun, Serge Lallemand, Arnaud Agranier, Diane Arcay, Franck Audemard, Marie-Odile Beslier, Milton Boucard, Mélody Philippon, Jean-Jacques Cornée, Maud Fabre, Aurélien Gay, David Graindorge, Arnauld Heuret, Frauke Klingelhoefer, Mireille Laigle, Jean-Len Léticée, Deny Malengros, Boris Marcaillou, Bernard Mercier de Lepinay, Philippe Münch, Emilien Oliot, Davide Oregioni, Crelia Padron, Frédéric Quillévéré, Gueorgui Ratzov, Laure Schenini, and Ben Yates.

References

Afilhado, A., Moulin, M., Aslanian, D., Schnürle, P., Klingelhoefer, F., Nouzé, H., et al. (2015). Deep crustal structure across a young passive margin from wide-angle and reflection seismic data (The SARDINIA Experiment) – II. Sardinia's margin. *Bulletin de la Societe Geologique de France*, *186*(4–5), 331–351.

Aïdi, C., Beslier, M. O., Yelles-Chaouche, A. K., Klingelhoefer, F., Bracene, R., Galve, A., et al. (2018). Deep structure of the continental margin and basin off Greater Kabylia, Algeria–New insights from wide-angle seismic data modeling and multichannel seismic interpretation. *Tectonophysics*, *728*, 1–22.

Aitken, T., Mann, P., Escalona, A., & Christeson, G. L. (2011). Evolution of the Grenada and Tobago basins and implications for arc migration. *Marine and Petroleum Geology*, *28*(1), 235–258. https://doi.org/10.1016/j.marpetgeo.2009.10.003

Allen, R. W., Collier, J. S., Stewart, A. G., Henstock, T., Goes, S., & Rietbrock, A. (2019). The role of arc migration in the development of the Lesser Antilles: A new tectonic model for the Cenozoic evolution of the eastern Caribbean. *Geology*, *47*, 891–895. https://doi.org/10.1130/G46708.1

Arnaiz-Rodríguez, M. S., & Audemard, F. (2018). Isostasy of the Aves Ridge and neighbouring basins. *Geophysical Journal International*, *215*, 2183–2197. https://doi.org/10.1093/gji/ggy401

Arnaiz-Rodríguez, M. S., Schmitz, M., & Audemard, F. (2016). La estructura cortical del arco de las Antillas Menores estimada a partir de la técnica de funciones receptoras. *Revista Mexicana de Ciencias Geológicas*, *33*(3), 286–296.

Audemard, F. A. (1993). Néotectonique, Sismotectonique et Aléa Sismique du Nord-ouest du Vénézuéla (Système de failles d'Oca–Ancón). PhD thesis (pp. 369). France: Université Montpellier II.

Audemard, F. A. (1998). Evolution Géodynamique de la Façade Nord Sud-américaine: Nouveaux apports de l'Histoire Géologique du Bassin de Falcón, Vénézuéla. 1995 Proceedings XIV Caribbean Geological Conference, Trinidad, 2, 327–340.

Audemard, F. A. (2009). Key issues on the post-Mesozoic southern Caribbean plate boundary. In K. H. James, M. A. Lorente, & J. Pindell (Eds.), Origin and evolution of the Caribbean plate. (Vol. 328. pp. 567–584) Geological Society, London, Special Publications. https://doi.org/10.1144/SP328.23

Badji, R., Charvis, P., Bracene, R., Galve, A., Badsi, M., Ribodetti, A., et al. (2015). Geophysical evidence for a transform margin offshore Western Algeria: a witness of a subduction-transform edge propagator?. *Geophysical Journal International*, *200*(2), 1029–1045.

Basile, C., Mascle, J., Sage, F., Lamarche, G., & Pontoise, B. (1996). *Pre-cruise and site surveys: A synthesis of marine geological and geophysical data on the Côte d'Ivoire-Ghana transform margin*.

Bauer, K., Neben, S., Schreckenberger, B., Emmermann, R., Hinz, K., Fechner, N., et al. (2000). Deep structure of the Namibia continental margin as derived from integrated geophysical studies. *Journal of Geophysical Research*, *105*(B11), 25829–25853. https://doi.org/10.1029/2000JB900227

Benes, V., & Scott, S. D. (1996). Oblique rifting in the Havre Trough and its propagation into the continental margin of New Zealand: Comparison with analogue experiments. *Marine Geophysical Researches*, *18*(2–4), 189–201.

Biari, Y., Klingelhoefer, F., Sahabi, M., Aslanian, D., Schnurle, P., Berglar, K., et al. (2015). Tectonophysics deep crustal structure of the North-West African margin from combined wide-angle and reflection seismic data (MIRROR seismic survey). *Tectonophysics*, *656*, 154–174. https://doi.org/10.1016/j.tecto.2015.06.019

Bird, D. E., Hall, S. A., Casey, J. F., & Millegan, P. S. (1999). Chapter 15 Tectonic evolution of the grenada basin. In P. Mann (Ed.), Sedimentary basins of the world. (Vol. 4, pp. 389–416) Elsevier, Caribbean Basins. https://doi.org/10.1016/S1874-5997(99)80049-5

Boschman, L. M., van Hinsbergen, D. J., Torsvik, T. H., Spakman, W., & Pindell, J. L. (2014). Kinematic reconstruction of the Caribbean region since the Early Jurassic. *Earth-Science Reviews*, *138*, 102–136.

Bouysse, P. (1988). Opening of the Grenada back-arc Basin and evolution of the Caribbean plate during the Mesozoic and early Paleogene. *Tectonophysics*, *149*(1–2), 121–143. https://doi.org/10.1016/0040-1951(88)90122-9

Bouysse, P., Andreieff, P., Richards, M., Baubron, J.-C., Mascle, A., Maury, R. C., et al. (1985). Aves swell and northern Lesser Antilles ridge: rock dredging results from Arcante 3 cruise. In A. Mascle (Ed.), *Géodynamique des Caraïbes. Proc Symp Géodynamique des Caraïbes* (pp. 65–76). Paris: Technip.

Boynton, C. H., Westbrook, G. K., Bott, M. H. P., & Long, R. E. (1979). A seismic refraction investigation of crustal structure beneath the Lesser Antilles island arc. *Geophysical Journal of the Royal Astronomical Society*, *58*(2), 371–393. https://doi.org/10.1111/j.1365-246X.1979.tb01031.x

Brune, S., Popov, A. A., & Sobolev, S. V. (2012). Modeling suggests that oblique extension facilitates rifting and continental break-up. *Journal of Geophysical Research*, *117*(B8). https://doi.org/10.1029/2011JB008860

Bunce, E. T., Phillips, J. D., Chase, R. L., & Bowin, C. D. (1970). The Lesser Antilles arc and the eastern margin of the Caribbean sea. The Sea. (Vol. 4, pp. 359–385).

Burke, K. (1988). Tectonic evolution of the Caribbean. *Annual Review of Earth and Planetary Sciences*, *16*, 201–230, https://doi.org/10.1146/annurev.ea.16.050188.001221

Cannat, M., Manatschal, G., Sauter, D., & Peron-Pinvidic, G. (2009). Assessing the conditions of continental breakup at magma-poor rifted margins: What can we learn from slow spreading mid-ocean ridges?. *Comptes Rendus Geoscience*, *341*(5), 406–427.

Cannat, M., Sauter, D., Mendel, V., Ruellan, E., Okino, K., Escartin, J., et al. (2006). Modes of seafloor generation at a melt-poor ultraslow-spreading ridge. *Geology*, *34*(7), 605–608.

Charvis, P., Recq, M., Operto, S., & Brefort, D. (1995). Deep structure of the northern Kerguelen Plateau and hotspot-related activity. *Geophysical Journal International*, *122*(3), 899–924. https://doi.org/10.1111/j.1365-246X.1995.tb06845.x

Christensen, N. I., & Mooney, W. D. (1995). Seismic velocity structure and composition of the continental crust: A global view. *Journal of Geophysical Research*, *100*(B6), 9761–9788. https://doi.org/10.1029/95JB00259

Christeson, G. L., Goff, J. A., & Reece, R. S. (2019). Synthesis of oceanic crustal structure from two-dimensional seismic profiles. *Reviews of Geophysics*, *57*(2), 504–529.

Christeson, G. L., Mann, P., Escalona, A., & Aitken, T. J. (2008). Crustal structure of the Caribbean–Northeastern South America arc-continent collision zone. *Journal of Geophysical Research*, *113*(8), 1–19. https://doi.org/10.1029/2007JB005373

Clark, S. A., Zelt, C. A., Magnani, M. B., & Levander, A. (2008). Characterizing the Caribbean–South American plate boundary at 64°W using wide-angle seismic data. *Journal of Geophysical Research*, *113*, B07401. https://doi.org/10.1029/2007JB005329

Crawford, W. C., Hildebrand, J. A., Dorman, L. M., Webb, S. C., & Wiens, D. A. (2003). Tonga Ridge and Lau Basin crustal structure from seismic refraction data. *Journal of Geophysical Research*, *108*, 2195. https://doi.org/10.1029/2001JB001435

Dean, S. M., & Minshull, T. A. (2000). Deep structure of the ocean-continent transition in the southern Iberia Abyssal Plain from seismic refraction profiles. *The IAM-9 transect at 40ø20 ′ N*, *105*, 5859–5885.

Dean, S. M., Minshull, T. A., & Whitmarsh, R. B. (2008). Seismic constraints on the three-dimensional geometry of low-angle intracrustal reflectors in the Southern Iberia Abyssal Plain. *Geophysical Journal International*, *175*(2), 571–586. https://doi.org/10.1111/j.1365-246X.2008.03869.x

Donnelly, T. W. (1975). The geological evolution of the Caribbean and Gulf of Mexico—Some critical problems and areas. In A. E. M. Nairn, & F. G. Stehli (Eds.), *The Gulf of Mexico and the Caribbean* (pp. 663–689). Boston, MA: Springer US. https://doi.org/10.1007/978-1-4684-8535-6_15

Evain, M., Galve, A., Charvis, P., Laigle, M., Kopp, H., Bécel, A., et al. (2013). Structure of the Lesser Antilles subduction forearc and backstop from 3D seismic refraction tomography. *Tectonophysics*, *603*, 55–67.

Ewing, J. I., Officer, C. B., Johnson, H. R., & Edwards, R. S. (1957). Geophysical investigations in the eastern Caribbean: Trinidad shelf, tobago trough, barbados ridge, Atlantic Ocean. *Bulletin of the Geological Society of America*, *68*(7), 897–912. https://doi.org/10.1130/0016-7606(1957)68[897:GIITEC]2.0.CO;2

Fox, P. J., Schreiber, E., & Heezen, B. C. (1971). The geology of the Caribbean crust: Tertiary sediments, granitic and basic rocks from the Aves ridge. *Tectonophysics*, *12*(2), 89–109. https://doi.org/10.1016/0040-1951(71)90011-4

Franke, D., Ladage, S., Schnabel, M., Schreckenberger, B., Reichert, C., Hinz, K., et al. (2010). Birth of a volcanic margin off Argentina, South Atlantic. *Geochemistry, Geophysics, Geosystems*, *11*, Q0AB04. https://doi.org/10.1029/2009GC002715

Funck, T., Jackson, H. R., Louden, K. E., Dehler, S. A., & Wu, Y. (2004). Crustal structure of the northern Nova Scotia rifted continental margin (eastern Canada). *Journal of Geodynamics*, *109*, 1–19. https://doi.org/10.1029/2004JB003008

Gailler, A., Klingelhoefer, F., Olivet, J. L., Aslanian, D., & Technical, O. B. S. (2009). Crustal structure of a young margin pair: New results across the Liguro–Provencal Basin from wide-angle seismic tomography. *Earth and Planetary Science Letters*, *286*(1–2), 333–345.

Garrocq, C., Lallemand, S., Marcaillou, B., Lebrun, J.-F., Padron, C., Klingelhoefer, F., et al. (2021). Genetic relations between the Aves Ridge and the Grenada back-arc Basin, East Caribbean Sea. *Journal of Geophysical Research: Solid Earth*, *126*, e2020JB020472. https://doi.org/10.1029/2020jb020466

González, O., Clouard, V., Tait, S., & Panza, G. (2018). S-wave velocities of the lithosphere-asthenosphere system in the Lesser Antilles from the joint inversion of surface wave dispersion and receiver function analysis. *Tectonophysics*, *734–735*, 1–15. https://doi.org/10.1016/j.tecto.2018.03.021

Hirn, A. (2001). *SISMANTILLES 1 cruise*. RV Le Nadir. https://doi.org/10.17600/1080060

Holbrook, W. S., Larsen, H. C., Korenaga, J., Dahl- Jensen, T., Reid, I. D., Kelemen, P. B., et al. (2001). Mantle thermal structure and active upwelling during continental breakup in the North Atlantic. *Earth and Planetary Science Letters*, *190*(3–4), 251–266.ISSN 0012-821X. https://doi.org/10.1016/S0012-821X(01)00392-2

Hotta, H. (1979). Stability of crust-mantle structures and tectonics of the island arc and trench system. *Journal of Physics of The Earth*, *18*, 79–113.

Jagoutz, O., Muntener, O., Manatschal, G., Rubatto, D., Péron-Pinvidic, G., Turrin, B. D., et al. (2007). The rift-to-drift transition in the North Atlantic: A stuttering start of the MORB machine?. *Geology*, *35*(12), 1087–1090.

Jurdy, D. M., & Stefanick, M. (1983). Flow models for back-arc spreading. *Tectonophysics*, *99*(2–4), 191–206.

Kearey, P. (1974). Gravity and seismic reflection investigations into the crustal structure of the Aves Ridge, eastern Caribbean. *Geophysical Journal of the Royal Astronomical Society*, *38*(3), 435–448. https://doi.org/10.1111/j.1365-246X.1974.tb05423.x

Klingelhoefer, F., Badji, R., Charvis, P., Leprêtre, A., Déverchère, J., Graindorge, D., et al. (2015). *Comparaison entre la structure profonde de la marge Algérienne et du Golfe de Lion, JST 10 de la Sonatrach, Oran, Algeria*.

Klingelhoefer, F., Evain, M., Afilhado, A., Rigoti, C., Loureiro, A., Alves, D., et al. (2014). Imaging proto-oceanic crust off the Brazilian Continental Margin. *Geophysical Journal International*, *200*(1), 471–488.

Kodaira, S., Noguchi, N., Takahashi, N., Ishizuka, O., & Kaneda, Y. (2010). Evolution from fore-arc oceanic crust to island arc crust: A seismic study along the Izu-Bonin fore arc. *Journal of Geophysical Research*, *115*(B9). https://doi.org/10.1029/2009JB006968

Kodaira, S., Sato, T., Takahashi, N., Miura, S., Tamura, T., Tatsumi, Y., et al. (2007). New seismological constraints on growth of continental crust in the Izu-Bonin intra-oceanic arc. *Geology*, *35*(11), 1031–1034. https://doi.org/10.1130/G23901A.1

Kopp, H., Weinzierl, W., Becel, A., Charvis, P., Evain, M., Flueh, E. R., et al. (2011). Deep structure of the central Lesser Antilles Island Arc: Relevance for the formation of continental crust. *Earth and Planetary Science Letters*, *304*(1–2), 121–134.

Laigle, M., Hirn, A., Sapin, M., Bécel, A., Charvis, P., Flueh, E., et al. (2013). Seismic structure and activity of the north-central Lesser Antilles subduction zone from an integrated approach: Similarities with the Tohoku forearc. *Tectonophysics*, *603*, 1–20. https://doi.org/10.1016/j.tecto.2013.05.043

LASE Study Group. (1986). Deep structure of the US East Coast passive margin from large aperture seismic experiments (LASE). *Marine and Petroleum Geology*, *3*(3), 234–242.

Laurencin, M., Graindorge, D., Klingelhoefer, F., Marcaillou, B., & Evain, M. (2018). Influence of increasing convergence obliquity and shallow slab geometry onto tectonic deformation and seismogenic behavior along the Northern Lesser Antilles zone. *Earth and Planetary Science Letters*, *492*, 59–72. https://doi.org/10.1016/j.epsl.2018.03.048

Laurencin, M., Marcaillou, B., Graindorge, D., Klingelhoefer, F., Lallemand, S., Laigle, M., et al. (2017). The polyphased tectonic evolution of the Anegada Passage in the northern Lesser Antilles subduction zone. *Tectonics*, *36*(5), 945–961. https://doi.org/10.1002/2017TC004511

Lebrun, J.-F., & Lallemand, S. E. (2017). *GARANTI cruise*. RV L'Atalante. https://doi.org/10.17600/17001200

Leprêtre, A., Klingelhoefer, F., Graindorge, D., Schnurle, P., Beslier, M. O., Yelles, K., et al. (2013). Multiphased tectonic evolution of the Central Algerian margin from combined wide-angle and reflection seismic data off Tipaza, Algeria. *Journal of Geophysical Research: Solid Earth*, *118*, 3899–3916. https://doi.org/10.1002/jgrb.50318

Louden, K. E. (1980). The crustal and lithospheric thicknesses of the Philippine Sea as compared to the Pacific. *Earth and Planetary Science Letters*, *50*(1), 275–288.

Ludwig, W. J., Nafe, J. E., & Drake, C. L. (1970). Seismic refraction. *Sea*, *4*, 53–84.

Lutter, W. J., & Nowack, R. L. (1990). Inversion for crustal structure using reflections from the PASSCAL Ouachita experiment. *Journal of Geophysical Research*, *95*, 4633–4646. https://doi.org/10.1029/JB095iB04p04633

Malfait, B. T., & Dinkelman, M. G. (1972). Circum-Caribbean tectonic and igneous activity and the evolution of the Caribbean plate. *GSA Bulletin*, *83*, 251–272. https://doi.org/10.1130/0016-7606(1972)83[251:CTAIAA]2.0.CO;2

Mascle, J., & Blarez, E. (1987). Evidence for transform margin evolution from the Ivory Coast–Ghana continental margin. *Nature*, *326*(6111), 378–381.

Melekhova, E., Schlaphorst, D., Blundy, J., Kendall, J.-M., Clare, C., McCarthy, A., et al. (2019). Lateral variation in crustal structure along the Lesser Antilles arc from petrology of crustal xenoliths and seismic receiver functions. *Earth and Planetary Science Letters*, *516*, 12–24. https://doi.org/10.1016/j.epsl.2019.03.030

Moulin, M., Klingelhoefer, F., Afilhado, A., Aslanian, D., Schnurle, P., Nouzé, H., et al. (2015). Deep crustal structure across a young passive margin from wide-angle and reflection seismic data (The SARDINIA Experiment) – I. Gulf of Lion's margin. *Bulletin de la Societe Geologique de France*, *186*(4–5), 309–330.

Museur, T., Graindorge, D., Klingelhoefer, F., Roest, W. R., Basile, C., Loncke, L., & Sapin, F. (2020). Deep structure of the Demerara Plateau: From a volcanic margin to a Transform Marginal Plateau. *Tectonophysics*, 228645. https://doi.org/10.1016/j.tecto.2020.228645

Neill, I., Kerr, A. C., Hastie, A. R., Stanek, K.-P., & Millar, I. L. (2011). Origin of the Aves Ridge and Dutch-Venezuelan Antilles: Interaction of the Cretaceous "Great Arc" and Caribbean-Colombian Oceanic Plateau? *Journal of the Geological Society*, *168*, 333–347.

Officer, C. B., Ewing, J. I., Edwards, R. S., & Johnson, H. R. (1957). Geophysical investigations in the eastern Caribbean: Venezuelan basin, Antilles island arc, and Puerto Rico trench. *Geological Society of America Bulletin*, *68*(3), 359–378.

Officer, C., Ewing, J., Hennion, J., Harkinder, D., & Miller, D. (1959). Geophysical investigations in the eastern Caribbean–summary of the 1955 and 1956 cruises. *Physics and Chemistry of the Earth*, *3*, 17–109. https://doi.org/10.1016/0079-1946(59)90004-7

Paulatto, M., Laigle, M., Galve, A., Charvis, P., Sapin, M., Bayrakci, G., et al. (2017). Dehydration of subducting slow-spread oceanic lithosphere in the Lesser Antilles. *Nature Communications*, *8*(May), 1–11. https://doi.org/10.1038/ncomms15980

Pindell, J. L., & Barrett, S. F. (1990). Geological evolution of the Caribbean region; A plate-tectonic perspective. In G. Dengo, & J. E. Case (Eds.), *The Caribbean region, Guatemala City, Guatemala* (pp. 405–432). Geological Society of America. https://doi.org/10.1130/DNAG-GNA-H.405

Pindell, J. L., & Kennan, L. (2009). Tectonic evolution of the Gulf of Mexico, Caribbean and northern South America in the mantle reference frame: An update. In K. H. James, M. A. Lorente, & J. L. Pindell (Eds.), The origin and evolution of the Caribbean plate (Vol. 328, pp. 1–55). Geological Society, London, Special Publications.

Reuber, K. R., Pindell, J., & Horn, B. W. (2016). Demerara Rise, offshore Suriname: Magma-rich segment of the Central Atlantic Ocean, and conjugate to the Bahamas hot spot. *Interpretation*, *4*, T141–T155. https://doi.org/10.1190/INT-2014-0246.1

Sallarès, V., Charvis, P., Flueh, E. R., & Bialas, J. (2003). Seismic structure of Cocos and Malpelo Volcanic Ridges and implications for hot spot-ridge interaction. *Journal of Geophysical Research*, *108*(B12), 1–21. https://doi.org/10.1029/2003jb002431

Sallarès, V., Martínez-Loriente, S., Prada, M., Gràcia, E., Ranero, C., Gutscher, M. A., et al. (2013). Seismic evidence of exhumed mantle rock basement at the Gorringe Bank and the adjacent Horseshoe and Tagus abyssal plains (SW Iberia). *Earth and Planetary Science Letters*, *365*, 120–131. https://doi.org/10.1016/j.epsl.2013.01.021

Sauter, D., Cannat, M., Rouméjon, S., Andreani, M., Birot, D., Bronner, A., et al. (2013). Continuous exhumation of mantle-derived rocks at the Southwest Indian Ridge for 11 million years. *Nature Geoscience*, *6*(4), 314–320.

Schellart, W. P., Lister, G. S., & Jessell, M. W. (2002). Analogue modelling of asymmetrical back-arc extension. *Journal of the Virtual Explorer*, *7*, 25–42.

Schlaphorst, D., Melekhova, E., Kendall, J.-M., Blundy, J., & Latchman, J. L. (2018). Probing layered arc crust in the Lesser Antilles using receiver functions. *Royal Society Open Science*, *5*, 180764. https://doi.org/10.1098/rsos.180764

Sclater, J. G., Karig, D., Lawver, L. A., & Louden, K. (1976). Heat flow, depth, and crustal thickness of the marginal basins of the south Philippine Sea. *Journal of Geophysical Research*, *81*(2), 309–318. https://doi.org/10.1029/JB081i002p00309

Sevilla, W. I., Ammon, C. J., Voight, B., & De Angelis, S. (2010). Crustal structure beneath the Montserrat region of the Lesser Antilles island arc. *Geochemistry, Geophysics, Geosystems*, *11*. https://doi.org/10.1029/2010GC003048

Shillington, D. J., Van Avendonk, H. J. A., Holbrook, W. S., Kelemen, P. B., & Hornbach, M. J. (2004). Composition and structure of the central Aleutian island arc from arc-parallel wide-angle seismic data. *Geochemistry, Geophysics, Geosystems*, *5*(10). https://doi.org/10.1029/2004GC000715

Sibuet, J. C., Letouzey, J., Barbier, F., Charvet, J., Foucher, J. P., Hilde, T. W., et al. (1987). Back arc extension in the Okinawa Trough. *Journal of Geophysical Research*, *92*(B13), 14041–14063. https://doi.org/10.1029/JB092iB13p14041

Smith, D. (2013). Tectonics: Mantle spread across the sea floor. *Nature Geoscience*, *6*(4), 247–248.

R. C. Speed, P. L. Smith-Horowitz, K. S. Perch-Nielsen, J. B. Saunders, & A. B. Sanfilippo (Eds.), (1993). Southern lesser Antilles arc platform: Pre-late Miocene stratigraphy, structure, and tectonic evolution. (Vol. *277*, pp. 98). Geological Society of America Special Paper.

Speed, R. C., & Walker, J. A. (1991). Oceanic crust of the Grenada Basin in the Southern Lesser Antilles Arc Platform. *Journal of Geophysical Research*, *96*, 3835–3851. https://doi.org/10.1029/90JB02558

Tomblin, J.-F. (1975). The Lesser Antilles and Aves ridge. *The ocean basins and margins: The Gulf of Mexico and the Caribbean* (pp. 467–500). Boston, MA: Springer US.

Van Avendonk, H. J., Davis, J. K., Harding, J. L., & Lawver, L. A. (2017). Decrease in oceanic crustal thickness since the breakup of Pangaea. *Nature Geoscience*, *10*, 58–61.

Van Avendonk, H. J. A., Holbrook, W. S., Nunes, G. T., Shillington, D. J., Tucholke, B. E., Louden, K. E., et al. (2006). Seismic velocity structure of the rifted margin of the eastern Grand Banks of Newfoundland, Canada. *Journal of Geophysical Research*, *111*, B11404. https://Doi.Org/10.1029/2005jb004156

Wadge, G. (1984). Comparison of volcanic production rates and subduction rates in the Lesser Antilles and Central America. *Geology*, *12*(9), 555–558. https://doi.org/10.1130/0091-7613(1984)12<555:COVPRA>2.0.CO;2

Westbrook, G. K. (1975). The structure of the crust and upper mantle in the region of Barbados and the Lesser Antilles. *Geophysical Journal of the Royal Astronomical Society*, *43*(1), 201–237. https://doi.org/10.1111/j.1365-246X.1975.tb00632.x

White, W., Copeland, P., Gravatt, D. R., and Devine, J. D. (2017). Geochemistry and geochronology of Grenada and Union islands, Lesser Antilles: The case for mixing between two magma series generated from distinct sources: *Geosphere*, *13*, 1359–1391, https://doi.org/10.1130/GES01414.1

White, R. S., Mckenzie, D. a N., & Nions, K. O. (1992). Crustal Thickness Earth of sediments acterised as normal ridge basalt (MORB) wide range of seismic velocities and The source composition and depth of melting of fled as the extrusive basaltic lavas and dykes formed at consistent and O • ions ' [1991]. *Journal of Geophysical Research*, *97*(B13), 19,683–19,715. https://doi.org/10.1016/j.csda.2008.03.004

Wu, Y., Louden, K. E., Funck, T., Jackson, H. R., & Dehler, S. A. (2006). Crustal structure of the central Nova Scotia margin off Eastern Canada. *Geophysical Journal International*, *166*(2), 878–906. https://doi.org/10.1111/j.1365-246x.2006.02991.x

Zelt, C. A. (1999). Modelling strategies and model assessment for wide-angle seismic traveltime data. *Geophysical Journal International*, *139*(1), 183–204. https://doi.org/10.1046/j.1365-246X.1999.00934.x

Zelt, C. A., & Smith, R. B. (1992). Seismic traveltime inversion for 2-D crustal velocity structure. *Geophysical Journal International*, *108*(1), 16–34. https://doi.org/10.1111/j.1365-246X.1992.tb00836.x